

NAO J-Th/
astro-ph/0005446

Neutrino Degeneracy and Decoupling: New Limits from Primordial Nucleosynthesis and the Cosmic Microwave Background

M. Orito¹, T. Kajino^{1,2,3}, G. J. Mathews^{1,4}, and R. N. Boyd⁵

ABSTRACT

We reanalyze the cosmological constraints on the existence of a net universal lepton asymmetry and neutrino degeneracy. For sufficiently large degeneracy, neutrino decoupling can occur before various particles annihilate and even before the QCD phase transition. These decoupled neutrinos are therefore not heated as the particle degrees of freedom change. The resultant ratio of the relic neutrino-to-photon temperatures after e- annihilation can then be significantly reduced by more than a factor of two from that of the standard nondegenerate ratio. This changes the expansion rate and subsequent primordial nucleosynthesis, photon decoupling, and structure formation. In particular we analyze physically plausible lepton-asymmetric models with large and degeneracies together with a moderate e-degeneracy. We show that the nucleosynthesis by itself permits very large neutrino degeneracies 0: ϵ_e , ϵ_ν 40, 0: ϵ_e 1:4 together with large baryon densities $0:1 \approx h_{50}^2$ 1 as long as some destruction of primordial lithium is assumed. We also show that structure formation and the power spectrum of the cosmic microwave background allows for the possibility of an $\epsilon_e = 1$, $\epsilon_\nu = 0:4$, cosmological model for which there is both significant lepton asymmetry ($j_e = j_\nu = 11$) and a relatively large baryon density ($\epsilon_b = 0:06$). Our best-fit neutrino-degenerate, high-baryon-content models are mainly distinguished by a suppression of the second peak in the microwave background power spectrum. This is consistent with the latest high resolution data from BOOMERANG and MAXIMA-1.

Subject headings: cosmology: HBBN, lepton asymmetry, constraints on ϵ_e , ϵ_ν , LiBeB, b - cosmic microwave background

¹ National Astronomical Observatory, 2-21-1, Ossawa, Mitaka, Tokyo 181-8588, Japan

² Graduate University for Advanced Studies, Department of Astronomical Science, 2-21-1, Ossawa, Mitaka, Tokyo 181-8588, Japan

³ University of Tokyo, Department of Astronomy, 7-3-1 Hongo, Bunkyo-ku, Tokyo 113-0033, Japan

⁴ Center for Astrophysics, and Department of Physics, University of Notre Dame, Notre Dame, IN 46556

⁵ Department of Physics, Department of Astronomy, Ohio State University, Columbus, OH 43210

1. INTRODUCTION

The universe appears to be charge neutral to very high precision (Lyttleton & Bondi 1959). Hence, any universal net lepton number beyond the net baryon number must reside entirely within the neutrino sector. Since the present relic neutrino number asymmetry is not directly observable there is no experimental basis for postulating that the lepton number for each species is zero. It is therefore possible for the individual lepton numbers L_1 of the universe to be large compared to the baryon number of the universe, B , while the net total lepton number is small ($L \neq B$). Furthermore, it has been suggested that even if the baryon number asymmetry is small, total lepton number could be large in the context of the SU(5) and SO(10) Grand Unified Theories (GUT's) (Harvey & Kolb 1981; Fry & Hogan 1982; Dolgov & Kirilova 1991; Dolgov 1992). It has also been proposed recently (Casas, Cheng, & Germani 1999) that models based upon the Ack-Dine scenario of baryogenesis (Ack & Dine 1985) might generate naturally lepton number asymmetry which is seven to ten orders of magnitude larger than the baryon number asymmetry. Neutrinos with large lepton asymmetry and masses ~ 0.07 eV might even explain the existence of cosmic rays with energies in excess of the Greisen-Zatsepin-Kuzmin cutoff (Greisen 1966; Germani & Kusenko 1999). It is, therefore, equally important for both particle physics and cosmology to carefully scrutinize the limits which cosmology places on the allowed range of both the lepton and baryon asymmetries.

The consequences of a large lepton asymmetry and associated neutrino degeneracy for big bang nucleosynthesis (BBN) have been considered in many papers. Models with degenerate e (Wagoner, Fowler, & Hoyle 1967; Terasawa & Sato 1985, 1988; Scherrer 1983; Kajino & Orito 1998a), both e and ν (Yahil & Beaudet 1976; Beaudet & Goret 1976; Beaudet & Yahil 1977), and for three degenerate neutrino species (David & Reeves 1980; Olive et al. 1991; Kang & Steigman 1992; Starkman 1992; Kajino & Orito 1998b; Kim & Lee 1995; Kim, Kim & Lee 1998) have been analyzed. The effects of the degeneracy of electron type neutrinos on inhomogeneous BBN models were also considered in Kajino & Orito (1998a, 1998b). Constraints on lepton asymmetry also arise from the requirement that sufficient structure develop by the present time (Kang & Steigman 1992) and from the power spectrum of fluctuations in the cosmic microwave background temperature (Kinney & Riotto 1999; Lesgourgues & Pastor 1999; Hannestad 2000).

The present work differs from all of those listed above primarily in that we carefully examine models with large neutrino degeneracies such that the neutrinos may decouple before the annihilation of various particles and even before the QCD transition. The fact that neutrinos may decouple when there were many particle degrees of freedom causes the relic neutrino temperature to be much lower by simple entropy considerations. This allows for interesting regions of the model parameter space in which substantial lepton asymmetry and baryon density is possible while still satisfying the adopted abundance constraints from primordial nucleosynthesis. We also find that for decoupling temperatures just above the QCD epoch it is possible to find models in which the structure constraint and even the CMB power spectrum constraint can be marginally satisfied.

In this paper we investigate an extensive range of baryon and lepton asymmetries from which we deduce new cosmological constraints on the baryon and lepton content of the universe. We emphasize that previous studies of BBN and the CMB temperature fluctuations with highly degenerate neutrinos have not exhaustively scrutinized the important effect from the lower implied neutrino temperature when neutrinos decouple before various particle annihilations and/or the QCD epoch. We correctly take this into account using the best currently available data on particle degrees of freedom in the early universe. We first discuss here how the observable BBN yields in a neutrino-degenerate universe impose bounds on the baryon and lepton asymmetries which still allow a large neutrino degeneracy and baryon density (even $b = 1$). We next examine other cosmological non-nucleosynthesis constraints, i.e. the cosmic microwave background (CMB) fluctuations and the time scale for development of structure. We show that these constraints can be marginally satisfied for a limited range of highly degenerate models from the fact the relic neutrino temperature is much lower than in the standard nondegenerate big bang. We also discuss how a determination of the neutrino degeneracy parameters could constrain the neutrino mass spectrum from the implied neutrino contribution to the closure density.

2. LEPTON ASYMMETRY & NEUTRINO DECOUPLING

In this section, we review the basic relations which define the magnitude of neutrino degeneracy and summarize the cosmological implications. Radiation and relativistic particles dominate the evolution of the early hot big bang. In particular, relativistic neutrinos with masses less than the neutrino decoupling temperature, $m < 0(T_D) \text{ MeV}$, contributed an energy density greater than that due to photons and charged leptons. Therefore, a small modification of neutrino properties can significantly change the expansion rate of the universe. The energy density of massive degenerate neutrinos and antineutrinos for each species is described by the usual Fermi-Dirac distribution functions f^+ and f^- ,

$$+\frac{1}{2} \int_0^{\infty} \frac{dp}{p^2} \frac{q}{p^2 + m^2} (f^+(p) + f^-(p)); \quad (1)$$

where, p denotes the magnitude of the 3-momentum, and m is the neutrino mass. Here and throughout the paper we use natural units ($\hbar = c = k_B = 1$). The distribution functions are

$$f^+(p) = \frac{1}{\exp(p=T) + 1}; \quad (2)$$

$$f^-(p) = \frac{1}{\exp(p=T + \eta) + 1};$$

where the degeneracy parameter η is defined in term of the neutrino chemical potential, $\eta = T$. It will have a nonzero value if a lepton asymmetry exists. Once the temperature drops sufficiently below the muon rest mass, say $T < 10 \text{ MeV}$, all charged leptons except for electrons

and positrons will have decayed away. Overall charge neutrality then demands that the difference between the number densities of electrons and positrons equal the proton number density. Hence, any electron degeneracy is negligibly small.

The net lepton asymmetry L of the universe can then be expressed as

$$L = \frac{\sum_{l=e,\bar{e}} L_l}{L_1};$$

$$L_1 = \frac{n_1 - n_{\bar{1}}}{n}; \quad (3)$$

to high accuracy. This is analogous to the baryon-to-photon ratio $(n_B - n_{\bar{B}})/n$. Here, n_1 ($n_{\bar{1}}$) are the number densities for each neutrino (antineutrino) species, n is the photon number density, and n_B ($n_{\bar{B}}$) is the (anti) baryon number density. After the epoch of e^-e^+ annihilation, the magnitudes of the lepton and baryon asymmetries are conserved. They are equal to the present value in the absence of any subsequent baryon and/or lepton number-violating processes.

Elastic scattering reactions, such as $e^-e^- + e^-e^- \rightarrow e^-e^- + e^-e^-$, keep the neutrinos in kinetic equilibrium. Annihilation and creation processes which can change their number density, like $e^-e^- \rightarrow \gamma + \gamma$, $e^-e^- \rightarrow p + \bar{p}$, etc, maintain the neutrinos in chemical equilibrium. When the rates for these weak interactions become slower than the Hubble expansion rate, neutrinos decouple and begin a "free expansion". Their number densities continue to diminish as $1=R^3$ and their comoving redshift by a factor $1=R$, where R is the cosmic scale factor. However, this decoupling has no effect on the shape of the distribution functions. Relativistic neutrinos and antineutrinos continue to be described by the Fermi-Dirac distributions of Eq. (2). Since the individual lepton number is believed to be conserved, the degeneracy parameters η_l remain constant after decoupling.

When one estimates the present density of relic neutrinos one must consider the effect of the changing number of degrees of freedom for the remaining interacting particles. For example, once the neutrinos are totally decoupled, they are not heated by subsequent pair annihilations. Hence, their temperature T_ν is lower than the temperature T_γ of photons (and any other electromagnetically interacting particles) by a factor $y = T_\nu/T_\gamma$. In the standard non-degenerate cosmology, with three flavors of massless, non-degenerate neutrinos which decouple just before the e^-e^+ pair annihilation epoch, the present ratio of the neutrino to photon temperatures is given by $y = (4=11)^{1/3}$.

Neutrinos and antineutrinos drop out of thermal equilibrium with the background thermal plasma at a decoupling temperature T_D , approximately given by the temperature at which ratio of the weak reaction rate, Γ_W , to the expansion rate, H , falls below unity. Significant neutrino degeneracy will cause the weak reaction rate, Γ_W , to be slower because the neutrino final states are occupied (Kang & Steigman 1992; Freese, Kolb, & Turner 1983). At the same time, the universal expansion in neutrino-degenerate models is more rapid because of the higher neutrino mass-energy density which pushes up the decoupling temperature. Both of these effects cause decoupling to

occur sooner and at a much higher temperature than in the non-degenerate case.

We have calculated the weak rate, Γ , for processes which can change neutrino number densities (e.g., $\nu + \bar{\nu} \rightarrow e + \bar{e}$) taking into account the neutrino degeneracies as well as the finite temperature corrections to the mass of the electron and photon (Fornengo, Kam, & Song 1997). The resultant neutrino decoupling temperatures for chemical equilibrium in the non-degenerate case are

$$\begin{aligned} T_D(\nu_e = 0) &= 2.93 \text{ MeV for } e; \\ T_D(\nu_\mu = 0) &= 5.45 \text{ MeV for } \mu; \end{aligned} \quad (4)$$

Figure 1 shows the decoupling temperature for the three neutrino species as a function of the degeneracy parameter. Differences in the temperatures relate to different reaction rates for the different neutrino species. Our results for the decoupling temperature at moderate neutrino degeneracies are in excellent agreement with those of Kang & Steigman (1992). However, we find slightly lower values for the ν_τ at which $T_D(\nu_\tau)$ is above the muon annihilation epoch.

One does not need to increase the temperature by much before heating by annihilations becomes a factor in the relic neutrino temperature. For illustration, Figure 2 shows the ratio of muon to photon energy densities as a function of temperature in units of the muon rest mass $m_\mu = 105 \text{ MeV}$. A similar curve could be drawn for any massive species. One can see that even at a temperature of only 20% of the muon rest mass, muons still contribute about 10% of the mass energy density and hence can affect the ratio of the photon to neutrino temperature as these remaining muons annihilate. Combining Figures 1 and 2, one can see that even for a degeneracy parameter of $\zeta = 6$, the decoupling temperature is at 20% of m_μ . For the case of highly degenerate neutrinos ($\zeta_e > 9.9$, and $\zeta_\mu > 8.7$), $T_D(\nu_\tau)$ can exceed the muon rest energy and even the QCD phase transition temperature.

If the neutrinos decouple early, they are not heated as the number of particle degrees of freedom change. Hence, the ratio of the neutrino to photon temperatures, $T_\nu = T_\mu$, is reduced. The computation of the ratio of the final present neutrino temperature to the photon temperature is straightforward. Basically, since the universe is a closed system, the relativistic entropy is conserved within a comoving volume. That is;

$$R^3 s = \text{Constant}; \quad (5)$$

where the entropy density s is defined,

$$s = \frac{\sum_i (g_i + p_i) \ln g_i}{T} = \frac{2}{45} g_{\text{eff}}^2 T^3; \quad (6)$$

and the sum is over all species present. Since the mass-energy is dominated by relativistic particles s can be written in terms of the effective number of particle degrees of freedom,

$$g_{\text{eff}} = \sum_{i=\text{bosons}}^X g_i \left(\frac{T_i}{T} \right)^3 + \frac{7}{8} \sum_{i=\text{fermions}}^X g_i \left(\frac{T_i}{T} \right)^3; \quad (7)$$

As each species annihilates, sR^3 to remains constant. Therefore, the temperature of the remaining species increases by a factor of $(g_{\text{eff}}^{\text{before}} = g_{\text{eff}}^{\text{after}})^{1/3}$. This accounts for the usual heating of photons relative to neutrinos due to pair annihilations by a factor of $(11=4)^{1/3}$. Note, that in the computation g_{eff} from equations 6 and 7 it is important to evaluate the energy densities continuously (cf. Figure 2) and not simply assume abrupt annihilation as the temperature approaches the rest energy of each particle as has sometimes been done.

Figure 3 shows g_{eff} as a function of temperature from 1 MeV to 1 TeV. To construct this figure we have included: (1) meson annihilations (, , , !, ;⁰); (5) lepton annihilations (e, , , e, ,); (2) a QCD phase transition at 150 MeV (u;d;gluon); (3) s-quarks (with $m_s = 120$ MeV); (4) c-quarks (with $m_c = 1200$ MeV); (6) b-quarks (with $m_b = 4250$ MeV); (7) W, Z-bosons (with $m_Z = 80$ GeV); and (8) t-quarks (with $m_t = 173$ GeV).

One can see from this figure that if neutrinos decouple before the QCD phase transition, the heating of photons increases by as much as a factor of $33.25^{1/3} = 3.2$. The higher the decoupling temperature, the more the photons are heated relative to the neutrinos. For example, with > 160 ,

$$\frac{T}{T_{\text{decoupling}}} < 0.43 \quad \frac{4}{11}^{1/3} : \quad (8)$$

Figure 4 shows the final ratio of neutrino temperature today to that of the standard non-degenerate big bang for three neutrino flavors. For all three neutrino flavors the temperature begins to decrease relative to the standard value for a degeneracy parameter as small as 5. This is because some relic pairs are still present even at temperatures well below the muon rest energy (cf. Figure 2). The first neutrino species to be affected as the degeneracy increases are the and . They decouple at a higher temperature than ν_e even in the standard nondegenerate big bang because the electrons continue to experience charged-current interactions to lower temperature.

The muon neutrinos exhibit a slightly different behavior than for degeneracy parameters > 5 because the density is large enough at the decoupling temperature for charged-current interactions to be significant. This maintains equilibrium to somewhat lower temperatures even for degenerate neutrinos. This causes the decoupling temperature to be lower (cf. Figure 1) and the relic temperature to be slightly higher than the temperature for degeneracy parameters between 5 and 9.

The biggest drop in temperature for all three neutrino flavors occurs for 10. This corresponds to a decoupling temperature above the cosmic QCD phase transition. The low temperature is the result of the decrease in particle degrees of freedom during this phase transition. This discontinuity will have important consequences in the subsequent discussions.

3. PRIMORDIAL NUCLEOSYNTHESIS

Although the homogeneous BBN model has provided strong support for the standard, hot big bang cosmology, possible conflicts exist between the predictions of BBN abundances as the astronomical data have become more precise in recent years. One difficulty has been imposed by recent detections of a low deuterium abundance (Burles & Tytler 1998a; Burles & Tytler 1998b, see also Levshakov, Tytler, & Burles 1999) in Lyman- absorption systems along the line of sight to high redshift quasars. The low D/H favors a high baryon content universe and a high primordial ^4He abundance, $Y_p > 0.244$. This is inconsistent with at least some of the reported constraints from measurements of a low primordial abundance of ^4He , $Y_p = 0.235 \pm 0.003$, in low-metallicity extragalactic H II regions (Olive & Steigman 1995; Steigman 1996; Hata et al. 1996; Olive, Steigman, & Skillman 1997; Kajino & Orito 1998a; Piemonti & Piemonti 2000). This situation is exacerbated by recent detailed analyses (Esposito et al. 1999; Lopez & Turner 1999) of the theoretical uncertainties in the weak interactions affecting the neutron to proton ratio at the onset of primordial nucleosynthesis. These results require a positive net correction to the theoretically determined ^4He mass fraction Y_p of $+0.004$ to $+0.005$ or $\sim 2\%$. We also note that the low deuterium abundance is marginally inconsistent with the ^7Li abundance inferred by measurements of lithium in Population II halo stars (Ryan et al. 1999; Kajino et al. 2000). Significant depletion of lithium from these stars, or a lower reaction rate for primordial lithium production may be required.

Another potential difficulty has been imposed by recent X-ray observations of rich clusters (White et al. 1993; White & Fabian 1995; David, Jones, & Forman 1995; Bahcall, Lubin, & Dorman 1995). The implied baryonic contribution to the closure density is $0.08 \pm h_{50}^{3=2} = 0.22$ (Tytler et al. 2000), where M is the total matter (dark plus visible) contribution, and h_{50} is the Hubble constant H_0 in units of $50 \text{ km s}^{-1} \text{ Mpc}^{-1}$. Consistency with the limits ($0.03 \pm h_{50}^{2=2} = 0.06$) from homogeneous BBN (Walker et al. 1991; Smith et al. 1993; Copi, Schramm & Turner 1995; Schramm & Mathews 1995; Olive, Steigman, & Walker 1999), then requires that $0.14 \pm M h_{50}^{1=2} = 0.75$. Hence, matter dominated cosmological models (for example with $H_0 = 75 \text{ km s}^{-1} \text{ Mpc}^{-1}$ and $M = 0.61$) can be in conflict with BBN.

Most previous works have only considered the effects of neutrino degeneracy on the light elements ^4He , D, and ^7Li . Recently, the predicted abundance of other elements such as ^6Li , ^9Be , and ^{11}B in a neutrino-degenerate universe were also studied (Kim & Lee 1995; Kim, Kim & Lee 1998). Here we investigate the effects of lepton asymmetry on predicted abundances of heavier elements (12 $\leq A \leq 18$) as well as these light elements.

Non-zero lepton numbers primarily affect nucleosynthesis in two ways (Wagoner, Fowler, & Hoyle 1967; Terasawa & Sato 1985; 1988; Scherrer 1983; Yahil & Beaudet 1976; Beaudet & Goret 1976; Beaudet & Yahil 1977; David & Reeves 1980; Olive et al. 1991; Kang & Steigman 1992; Starkman 1992; Kajino & Orito 1998a; Kim & Lee 1995; Kim, Kim & Lee 1998). First, degeneracy in any neutrino species leads to an increased universal expansion rate independently of

the sign of ϵ . As a result, the weak interactions that maintain neutrons and protons in statistical equilibrium decouple earlier. This effect alone would lead to an enhanced neutron-to-proton ratio at the onset of the nucleosynthesis epoch and increased ^4He production.

Secondly, a non-zero electron neutrino degeneracy can directly affect the equilibrium n/p ratio at weak-reaction freeze out. The equilibrium n/p ratio is related to the electron neutrino degeneracy by $n/p = \exp(-M/T_{n/p})$, where M is the neutron-proton mass difference and $T_{n/p}$ is the freeze-out temperature for the weak reactions converting protons to neutrons and vice versa. This effect leads to either increased or decreased ^4He production, depending upon the sign of L_e or ϵ .

There is also a third effect which we emphasize in this paper. As discussed in the previous section, $T = T_c$ can be reduced if the neutrinos decouple at an earlier epoch. This lower temperature reduces the energy density of the highly degenerate neutrinos during the BBN era, and hence, slows down the expansion of the universe. This leads to decreased ^4He production. We show in the next section that the allowed values for ϵ ; η ; and b which satisfy the light-element abundance constraints are significantly changed for large degeneracy ($\eta, b > 9$) compared to the results of previous studies.

3.1. Summary of Light-Element Constraints

The primordial light element abundances deduced from observations have been reviewed by a number of recent papers (Olive, Steigman, & Walker 1999; Nollett & Burles 2000; Steigman 2000; Tytler et al. 2000). There are several outstanding uncertainties. For primordial helium there is an uncertainty due to the fact that deduced abundances tend to reside in two possible values, one high and the other low. Hence, for ^4He we adopt a wide range:

$$0.226 \leq Y_p \leq 0.247:$$

For deuterium there is a similar possibility for either a high or low value. Here, however, we adopt the generally accepted low values of Tytler et al. (2000),

$$2.9 \times 10^{-5} \leq D/H \leq 4.0 \times 10^{-5}:$$

For primordial lithium there is some uncertainty from the possibility that old halo stars may have gradually depleted their primordial lithium. Because of this possibility we adopt the somewhat conservative constraint:

$$1.26 \times 10^{-10} \leq ^7\text{Li/H} \leq 3.5 \times 10^{-10}$$

4. Nucleosynthesis Results

As we shall see, the shifts in the relic neutrino temperature during primordial nucleosynthesis can dramatically affect the abundance yields (Kajino & Orito 1998b). We now explore the parameter space of neutrino degeneracy and baryon-to-photon ratio to reinvestigate the range of models compatible with the constraints from light element abundances.

For the present work we have applied a standard big bang code with all reactions updated up to $A = 18$. However, in the present discussion only reactions involving nuclei up to $A = 15$ are significant. In this way possible effects of lepton asymmetry on heavier element abundances could be analyzed along with the light elements. In this context a recent compilation of the nuclear reaction rates relevant to the production of ^{11}B (Orito, Kajino, & Oberhummer 1998) was useful because several important $\text{Li} + \text{Be} + \text{B}$ (α, x) and (n, γ) reaction rates in the literature sometimes differ from one another by 2-3 orders of magnitude. The calculated abundances of heavier elements based upon these rates can also differ from one another by 1-2 orders of magnitude. We carry out BBN calculations which include all of the recent compilations of reaction rates relevant to the production of isotopes including those that are heavier than ^6Li up to ^{18}O (i.e. Orito, Kajino, & Oberhummer 1998; Mohr, Hemandl, & Oberhummer 1999; Angulo et al. 1999; Hemandl et al. 1999; Wagoner et al. 1999; and any other previous estimates are considered).

We have explored a broad range of the parameter space of neutrino-degenerate models. The main effects of the inclusion of either or degeneracy on BBN is an enhancement of energy density of the universe. The values for and primarily affect the expansion rate. This means that and are roughly interchangeable as far as their effects are nucleosynthesis concerned. Furthermore, we expect that the net total lepton number is small though the lepton number for individual species could be large. Hence, it is perhaps most plausible to assume that the absolute values of j_e and j_ν are nearly equal. Therefore, in what follows, we describe results for $j_\nu = j_e$. This reduces the parameter space to three quantities: b , ϵ , and $j_\nu = j_e$.

The calculations were conducted out by first choosing a value for bh_{50}^2 . It is then necessary to find a value of ϵ for which the light element constraints can be satisfied for some value of j_ν .

As an illustration, Figure 5 shows a calculation of the helium abundance as a function of j_ν in a model with $bh_{50}^2 = 0.3$. It was found in this model that the helium constraint could be satisfied for ϵ in the range of 0.75 to 0.95. This figure is for $\epsilon = 0.8$. In this calculation, our results for $j_\nu < 10$ are consistent with those of Kang & Steigman (1992). Note, however, that the helium abundance is significantly changed at high values of j_ν , by taking into account the effect of the lower neutrino temperature during primordial nucleosynthesis. (See Figure 4.) This effect of varying $T_\nu = T_\text{b}$ for large j_ν on BBN has not been adequately explored in the previous studies.

Figure 6 illustrates the effects on the other light-element abundances for this particular

parameter set. This figure shows that for moderate values of η , the main effect is that weak reaction freeze-out occurs at a higher temperature. The resultant enhanced n/p ratio increases the abundances of the neutron-rich light elements, D, ^3H and ^7Li , while the ^7Be abundance decreases.

Regarding ^7Li and ^7Be abundances, the enhanced expansion rate from neutrino degeneracy affects the yield of $A = 7$ elements in two different ways. These elements are produced mainly by the nuclear electromagnetic capture reactions: $t(\gamma, n)$, ^7Li and $^3\text{He}(\gamma, n)$, ^7Be . Hence, the production of these elements begins at a later time and lower temperature than the other light elements because they require time for a significant build up of the reacting $A = 3$ and 4 elements. In a neutrino-degenerate universe, however, the increased expansion rate, hastens the freeze-out of these reactions from nuclear statistical equilibrium (NSE) resulting in reduced $A = 7$ yields relative to the nondegenerate case. However, the enhanced n/p ratio also increases the tritium abundance in NSE. This effect tends to offset the effect of rapid expansion on the production of ^7Li . The net result is more ^7Li production.

As in the case of primordial helium, there is a rapid change in nalyields once the and decoupling temperatures separately exceed the epoch of QCD phase transition. The ensuing lower neutrino temperature during primordial nucleosynthesis then resets the abundances to those of a lower effective degeneracy. The two discontinuities in Figure 6 correspond to the points at which the muon or tau neutrino decoupling temperature exceeds the QCD phase transition temperature.

Figure 7(a) summarizes the allowed regions of the η vs. η , plane based upon the various indicated light element constraints in a universe with $bh_{50}^2 = 0.1$. The usually identified allowed region (cf. Kohri, Kawasaki, & Sato 1997) for small η , $\eta < 0.3$ and $\eta < 2$ is apparent. Indeed, it has been argued (cf. Kohri, Kawasaki, & Sato 1997) that such degeneracy may be essential to explain the differences in the constraints from primordial helium and deuterium.

Figures 7(b) and 7(c) show the same plots, but for $bh_{50}^2 = 0.2$ and $bh_{50}^2 = 0.3$, respectively. In these two figures, new regions of the parameter space are evident. The decline in the primordial deuterium abundance for models in which $\eta > 10$ allows for new regions of the parameter space in which the light element constraints can be accommodated. This trend of a new allowed region for higher degeneracy persists as the baryon density is increased.

Figure 8 highlights the basic result of this study. For low bh_{50}^2 models, only the usual low values for η and η , are allowed. Between $bh_{50}^2 = 0.15$ and 0.3 , however, more than one allowed region emerges. For $bh_{50}^2 > 0.4$ only the large degeneracy solution is allowed. Neutrino degeneracy can even allow baryonic densities up to $bh_{50}^2 = 1$. This result has been noted previously (cf. Kang & Steigman 1992; Starkman 1992). What is different here is that the high bh_{50}^2 models are made possible for smaller values of η by careful accounting of the relic neutrino temperature. This suggests that baryons and degenerate neutrinos might provide a larger contribution to the universal closure density than has previously been assumed based upon light-element constraints from BBN.

Figure 9 summarizes the neutrino contribution to the closure density Ω_ν as a function of

neutrino degeneracy and mass. This figure assumes the plausible model of nearly degenerate and massless and negligible mass. For this figure refers to the combined contributions from both and . The contribution changes for large degeneracy due to the lower present-day neutrino temperature. This figure can be used to constrain the masses of the and neutrino types in different cosmological models. For example, if we assume a model with $bh_{50}^2 = 0.1$, $= 0.6$, and $= 0.3$, then we would find that the masses of both the and must be < 2 eV, if these two species are to provide the neutrino contribution to the closure density.

Figures 10-12 illustrate the elemental abundances in allowed models as a function of bh_{50}^2 . Figure 12 in particular allows us to consider whether there exists an abundance signature in other elements which might distinguish this new degenerate neutrino solution from standard BBN. For the most part the yields of the light and heavy species are similar to those of the standard non-degenerate big bang. However, the boron abundance exhibits an increase with baryon density due to alpha captures on ^7Li followed by a decrease due to reactions with ^{11}B . Similarly, the beryllium and ^6Li abundances exhibit some increase. Thus, in principle, an anomalously low boron abundance together with enhanced beryllium and ^6Li relative to that expected from the standard big bang might be a signature of neutrino-degenerate BBN.

5. OTHER COSMOLOGICAL CONSTRAINTS

We have seen that a new parameter space in the constraints from light elements on BBN emerges in neutrino-degenerate models just from the fact that the relic neutrino temperature is substantially diminished when degeneracy pushes neutrino decoupling to an earlier epoch. The viability of this solution requires large neutrino degeneracy. Hence it becomes necessary to reexamine constraints posed from other cosmological considerations.

5.1. Structure Formation

It has been argued (Kang & Steigman 1992) that large neutrino degeneracy is ruled out from the implied delay in galaxy formation in such a hot dark matter universe. This argument is summarized (Kang & Steigman 1992) as follows:

Neutrino degeneracy speeds up the expansion rate by a factor

$$S_0^2(\tau) = 1 + 0.135(F(\tau) - 3) - 0.135F(\tau); \quad (9)$$

where $F(\tau)$ is an effective energy density factor (Kang & Steigman 1992) for neutrinos. For massless neutrinos we have

$$F(\tau) = \frac{\sum_i X_i F(\tau_i)}{\sum_i X_i} = \frac{\sum_i \frac{T_i}{T_{\text{Nuc}}}^{-4}}{\sum_i \frac{T_i}{T_{\text{Nuc}}}} = 1 + \frac{15}{7} \frac{\sum_i \tau_i^{-4}}{\sum_i \tau_i^{-2}} + \frac{30}{7} \frac{\sum_i \tau_i^{-2}}{\sum_i \tau_i^{-2}}; \quad (10)$$

where $(T_i = T)_{\text{Nuc}}$ is the neutrino-to-photon temperature ratio before e pair annihilation. This ratio is unity in the standard model with little or no degeneracy.

With the expansion speeded up, the time of matter-radiation equality occurs at smaller redshift and there is less time for the growth of fluctuations. The redshift $z_{\text{eq}}(\nu)$ for matter-radiation equality for the neutrino degenerate universe can be written in terms of the redshift for a nondegenerate universe,

$$1 + z_{\text{eq}}(\nu) = S_0^2 (1 + z_{\text{eq}}(\nu = 0)); \quad (11)$$

For the present matter-dominated universe without neutrino degeneracy and $M \approx 1$ we have $1 + z_{\text{eq}}(\nu = 0) \approx 1.06 \cdot 10^4$ (Kang & Steigman 1992). Furthermore, one demands that the fluctuation amplitude $A(z)$ grows at least linearly with redshift, i.e. $A(z) \approx (1 + z_{\text{eq}})A(z_{\text{eq}})$. One also requires that the amplitude at least reaches unity by the present time,

$$\frac{1}{A(z_{\text{eq}})} \approx (1 + z_{\text{eq}}) \approx \frac{A(z = 0)}{A(z_{\text{eq}})} : \quad (12)$$

Thus, the requirement of sufficient growth in initial perturbations places a bound on the speed-up. Namely,

$$S_0^2 \approx \frac{1.06 \cdot 10^4}{1 + z_{\text{eq}}(\nu)} \approx 1.06 \cdot 10^4 A(z_{\text{eq}}) : \quad (13)$$

Then requiring that $A(z_{\text{eq}}) \approx 10^{-3}$ (Steigman & Turner 1985) leads to the constraint that $F(\nu) \approx 10.6 = 135 \cdot 79$.

Figure 13 shows the $F(\nu)$ and $F(\nu_i)$ calculated as a function of ν , for the allowed models of Figure 8. Since our interesting parameter regions in Figure 8 satisfy $\nu_e \approx \nu_i$, only ν_e contributes significantly to the total $F(\nu)$. Also shown are values of $F(\nu_i)$ if only one neutrino species was degenerate. The dashed line gives the constraint $F(\nu) \leq 79$ from Kang & Steigman (1992). For low values of ν , our $F(\nu_i)$ values are consistent with the constraint of Kang & Steigman (1992). However, as ν_i increases, our curves are lower due to the fact that we treat the annihilation epochs continuously (cf. Figure 4) rather than discretely, except for the QCD transition. By chance, our limit in the low degeneracy range for two degenerate neutrinos, i.e. $\nu_i < 6.9$ is identical to the single species limit of Kang & Steigman (1992). However, in addition we now find that there exists a new allowed region with $10 < \nu_i < 14.5$ for which this growth constraint is satisfied. This corresponds to allowed BBN models with a baryon fraction as large as $bh_{50}^2 < 0.25$ (cf. Figure 8). Note also that if only a single neutrino species were degenerate, then values of degeneracy up to $\nu_i < 20$ are allowed.

Cosmology also places a constraint on the neutrino mass in degenerate and nondegenerate hot-dark-matter (HDM) models. Indeed, at least some neutrino mass may presently be required to account for the observed power spectrum of galactic and microwave background structure. It has been argued (Primack et al. 1995) from considerations of structure formation in the early universe that two neutrino flavors (ν_e, ν_i) may have a rest mass of 2.4 eV, compatible with all neutrino oscillation experiments. This postulate solves the main problem of cold dark matter

(CDM) models, i.e. production of too much structure on small scales. However, the fact that the neutrinos in this model are at a much lower temperature may alter this constraint on the neutrino mass in degenerate models. It may therefore be necessary, for the mass of 2.4 eV to be recalculated, in the context of the modified neutrino temperature and number density in the leptonic asymmetric models discussed here (Bell, Foot, & Volkas 1998). Nevertheless, if we take 2.4 eV as the given mass of ν_1 and ν_2 , then from Figure 9 we would deduce that the maximum degeneracy for two species with this mass would correspond to $\nu_1 \approx 0.9$, $bh_{50}^2 \approx 0.1$, and $\nu_2 \approx 2.5$.

5.2. Cosmic Microwave Background Constraint

Perhaps, the most stringent remaining constraint on neutrino degeneracy comes from its effect on the cosmic microwave background. Several recent works (Kinney & Riotto 1999; Lesgourgues & Pastor 1999; Hannestad 2000) have shown that neutrino degeneracy can dramatically alter the power spectrum of the CMB. The essence of the constraint is that degenerate neutrinos increase the energy density in radiation at the time of photon decoupling in addition to delaying the time of matter-radiation energy-density equality as discussed above. One effect of this is to increase the amplitude of the first acoustic peak in the CMB power spectrum at $l = 200$. For example, based upon a χ^2 analysis (Lineweaver & Barbosa 1998) of 19 experimental points and window functions, Lesgourgues and Pastor (1999) concluded that $\nu_1 \approx 6$ for a single degenerate neutrino species.

However, in the existing CMB constraint calculations (Kinney and Riotto 1999; Lesgourgues and Pastor 1999; Hannestad 2000) only small degeneracy parameters with the standard relic neutrino temperatures were utilized in their derived constraint. Hence, the possible effects of a diminished relic neutrino temperature need to be reconsidered. To investigate this we have done calculations of the CMB power spectrum, $T^2 = 1/(1 + 1/C_{l=2})$ based upon the CMBFAST code of Seljak & Zaldarriago (1996).

We have explicitly modified this code to account for the contribution of massless degenerate neutrinos with a relic temperature ratio $y = T_{\nu}/T_{\text{rec}}$ as given in Figure 4. We only consider massless neutrinos here. For the optimum neutrino-degenerate models ($\nu_1 \approx 10$) and a neutrino contribution $\nu_1 \approx 0.3$ we deduce from the solid curve on Figure 9 that the neutrino mass is $m_{\nu_1} \approx 0.3$ eV and therefore unimportant during the photon decoupling. For massless neutrinos it can be proven (Lesgourgues & Pastor 1999) that the only effect of neutrino degeneracy is to increase the background pressure and energy density of relativistic particles (cf. Eqs. 1,2 and 10).

We have evaluated χ^2 fits to the CMB power spectrum, based upon the "radial compression" technique as described in Bond, Jaffe & Knox (2000). We have used the latest 69 observational points and window functions available from the web page given in that paper. The advantage of this approach is that the non-Gaussian nature of the experimental uncertainties in the power spectrum is correctly weighted in the evaluation of the χ^2 .

For the purposes of the present study, we take as a benchmark the "All" case best $t = 1$

model of Dodelson & Knox (2000) who derived cosmological parameters based upon this same data set and compression technique. Although there is some degeneracy in the cosmological parameters they deduced an optimum t to the power spectrum for $bh^2 = 0.019$, $H_0 = 65 \text{ km sec}^{-1} \text{ Mpc}^{-1}$, $\tau = 0.65$, $M = 0.35$, $\eta = 0.17$, and $n = 1.12$, where M is the total matter contribution, τ is the reionization parameter, and n is the "tilt" of the power spectrum. This benchmark is plotted as the dashed curve in Figure 14. For this case we find $\chi^2 = 101$. Note that our χ^2 is different from that quoted in Dodelson & Knox (2000) because we use different binning of the power spectrum]. For comparison the "radical compression" of the CMB data into 14 bins used in this work is also shown (Bond et al. 2000).

Rather than to do an exhaustive parameter search we have taken an approach similar to Lesgourges & Pastor (1999). That is, we fix several representative cosmological models and then study their goodness of t to the CMB data. The best case for large neutrino degeneracy will be for a value of the degeneracy parameter η , such that neutrino decoupling occurs just before the QCD phase transition. This is the value for which the relic neutrino energy density is a local minimum (cf. Figure 13). For the present work this corresponds to $\eta = 10.7$, $\tau_e = 0.58$, $bh_{50}^2 = 0.144$ models. In what follows we fix η , τ_e , and bh_{50}^2 at these values and refer to this as the large degeneracy model.

We have found [as did Lesgourges & Pastor (1999)] that the currently favored $\eta = 0.7$ models give a poor t to the data even with no degeneracy. Adding neutrino degeneracy to an $\eta = 0.7$ model only makes the t worse. The main problem is that the first acoustic peak increases in amplitude and moves to larger l . Hence, even though a local minimum develops for large degeneracy, the χ^2 is substantially increased and large neutrino degeneracy is probably ruled out for $\eta = 0.7$ models.

For smaller η a local minimum develops in the χ^2 for both small values of degeneracy $\eta = 1$ and large degeneracy $\eta = 10.7$. As pointed out in Lesgourges & Pastor (1999), the best case for neutrino degeneracy is with $\eta = 0$ models. However, those models are probably ruled out by observations of type Ia supernovae at high redshift (Gamovich, et al. 1998; Perlmutter et al. 1998a; Perlmutter et al. 1998b; Riess et al. 1998). At the 3 confidence level for $\eta = 1$ models, the type Ia Supernova data are consistent with $\eta = 0.7 - 0.3$. Hence, we take $\eta = 0.4$ as a plausible cosmological model which is marginally consistent with the type Ia results. Nevertheless, for purposes of illustration, we have also made a search for optimum parameters for matter dominated $\eta = 0, \eta = 1$ models.

The reason low η models are favored is that they shift the first acoustic peak back to lower l . Larger values of H_0 also slightly improve the t by shifting the first acoustic peak to lower l and decreasing the baryon density for fixed bh_{50}^2 which lowers the peak amplitude. We take $H_0 = 65 - 10$ ($h_{50} = 1.3 - 0.2$) as a reasonable range (Dodelson & Knox 2000), and therefore utilize $h_{50} = 1.5$ as the optimum Hubble parameter for the neutrino-degenerate models. This implies that $b = 0.064$ for the large degeneracy models. The ionization parameter does not particularly

help the t s as it mainly serves to decrease the amplitude of both the first and second peaks in the power spectrum. We therefore set $\tau = 0$ for the large degeneracy models. The only remaining adjustable parameter of the t s is then the tilt parameter n . Values of n slightly below unity also help with the amplitude and location of the first acoustic peak.

The solid line on Figure 14 shows a $\tau = 0.4$ model for which $n = 0.86$. For this $t \tau^2 = 11$ which makes this large degeneracy model marginally consistent with the data at a level of 3:3. The dotted line in Figure 14 shows the matter dominated $\tau = 0$ best fit model with $n = 0.94$. For this $t \tau^2 = 5$ which makes this large degeneracy model consistent with the data at the level of 2:2.

As can be seen from Figure 14, a model with large neutrino degeneracy seems marginally acceptable based upon the presently uncertain power spectrum. The main differences in the t s between the large degeneracy models and our adopted benchmark model are that the first peak is shifted to slightly higher l values and the second peak is somewhat suppressed. It thus becomes important to quantify the amplitude of the second peak in order to constrain the large degeneracy models proposed herein.

Indeed, after the present t s were completed a suppression of the second acoustic peak in the power spectrum has been recently reported in the high-resolution BOOMERANG (Bernardis, P. et al. 2000; Lange et al. 2000) and MAXIMA-1 (Hanany et al. 2000; Balbi et al. (2000)) results. We have not yet analyzed the goodness of t to these data as the experimental window functions are not yet available. In a subsequent paper we will examine the implications of those data in detail.

For purposes of illustration, however, we compare the t models of Figure 14 with the published BOOMERANG and MAXIMA-1 power spectra in Figure 15. Here one can clearly see that the suppression of the second acoustic peak in the observed power spectrum is consistent with our derived neutrino-degenerate models. In particular, the MAXIMA-1 results are in very good agreement with the predictions of the neutrino-degenerate cosmological models described herein. There is, however, a calibration uncertainty between these two sets (Hanany et al. 2000). If one only considers the BOOMERANG results alone, the diminished amplitude of the first acoustic peak probably tightens the constraint for low neutrino degeneracy models (cf. Hannestad 2000) although even for this set alone, a high degeneracy model is probably still acceptable (Lesgourges & Peloso 1999). It is clear, that these new data sets will substantially improve the goodness of t for the neutrino-degenerate models (Lesgourges & Peloso 1999). Moreover, both data sets seem to require an increase in the baryonic contribution to the closure density as allowed in our neutrino-degenerate models.

6. Conclusions

We have discussed how the relic neutrino temperature is substantially diminished in cosmological models with a large neutrino degeneracy. We have shown that all of the BBN

light-element abundance constraints (assuming some destruction of ^7Li) can be satisfied for cosmological models in which significant neutrino degeneracies and large values of bh^2 exist. The requirement that large scale structure can become nonlinear in sufficient time can also be satisfied for models with large neutrino degeneracy $10.7 < \eta < 14$ and $bh_{50}^2 < 0.25$. We have shown that even the constraint from neutrino degeneracy effects on fluctuations of the cosmological microwave background temperature may be marginally avoided for models with $\eta < 0.4$, $\eta = 10.7$, and bh_{50}^2 as large as 0.144.

At present, the power spectrum of the CMB is the most stringent constraint. Nevertheless, neutrino-degenerate models can be found which are marginally consistent at the 2-3 level. This tight constraint is due, at least in part, to a suppression of the second acoustic peak in the spectrum. It is therefore encouraging that the recent BOOMERANG and MAXIMA-1 results suggest that such a suppression in the second acoustic peak may indeed occur consistent with the expectations of the large neutrino degeneracy, high b models proposed here.

Thus, high resolution microwave background observations become even more important as a means to quantify the limits to (or existence of) possible cosmological neutrino degeneracy. Based upon the current analysis, we conclude that all of the cosmological constraints on large neutrino degeneracy are marginally satisfied when a careful accounting of the neutrino decoupling and relic neutrino temperature is made. It will, therefore, be most interesting to see what further constraints can be placed on this possibility from the soon to be available space-based high resolution CMB observations such as the NASA MAP and ESA Planck missions.

One of the authors (GJM) wishes to acknowledge the hospitality of the National Astronomical Observatory of Japan where much of this work was done. This work has been supported in part by the Grant-in-Aid for Scientific Research (10640236, 10044103, 11127220, 12047233) of the Ministry of Education, Science, Sports, and Culture of Japan, and also in part by NSF Grant PHY-9901241 at OSU) along with DOE Nuclear Theory Grant DE-FG 02-95-ER40394 at UND).

R E F E R E N C E S

Ack, I., & Dine, M. 1985, Nucl. Phys. B., 249, 361

Angulo, C. et al. (NACRE collaboration) 1999, Nucl. Phys. A., 656, 3

Bahcall, N. A., Lubin, L. M., & Dorman, V. 1995, ApJ, 447, L81

Balbi, A. et al. 2000, ApJL submitted, astro-ph/005124

Bell, N. F., Foot, R., & Volkas, R. R., 1998, Phys. Rev. D., 58, 105010

Beaudet, G., & Goret, P. 1976, A & A, 49, 415

Beaudet, G ., & Yahil, A . 1977, ApJ, 218, 253

Bernardls, P . et al. (Boomerang Collaboration) 2000, Nature, 404, 955

Bond, J. R ., Jaffe, A . H . & Knox, L . 2000, ApJ, 533, 19; data available from :
<http://www.cita.utoronto.ca/knox/radical.htm>

Burles, S . & Tytler, D . 1998a, ApJ, 499, 699

Burles, S . & Tytler, D . 1998b, ApJ, 507, 732

Casas, A ., Cheng, W . Y ., & Gelmini, G . 1999, Nucl Phys. B ., 538, 297

Copi, C . J ., Schramm, D . N ., & Turner, M . S . Science 1995 267 192; ApJL 455 95

David, Y ., & Reeves, H . 1980, Phil. Trans. Roy. Soc., A 296, 415

David, L . P ., Jones, C . J ., & Forman, W . 1995, ApJ, 445, 578

Dodelson, S . & Knox, L . 2000, Phys. Rev. Lett., 84, 3523

Dolgov, A . & Kirilova, D . P . J . 1991, Moscow Phys. Soc., 1, 217

Dolgov, A . 1992, Phys. Rep., 222, 309

Espósito, S ., Mangano, G ., Miele, G ., & Pisanti, O . 1999, Nucl Phys. B ., 540, 3

Freese, K ., Kolb, E . J ., & Turner, M . S . 1983, Phys. Rev. D ., 27, 1689

Fomengo, N ., Kim, C . W ., & Song, J ., 1997, Phys. Rev. D ., 56, 5123

Fry, J. N ., & Hogan, C . J . 1982, Phys. Rev. Lett., 49, 1873

Gamovich, P . M . et al. 1998, ApJ, 509, 74

Gelmini, G . & Kusenko, A . 1999, Phys. Rev. Lett., 82, 5202

Greisen, K . 1966, Phys. Rev. Lett., 16, 748

Haanestad, S . 2000, Phys. Rev. Lett., submitted, astro-ph/0005018

Hanany, S . et al. (MAXIMA-1 Collaboration) 2000, ApJL submitted, astro-ph/0005123

Harvey, J. A . & Kolb, E . W . 1981, Phys. Rev. D ., 24, 2090

Hata, N ., Scherrer, R . J ., Steigman, G ., Thomas, D . & Walker, T . P . 1996, ApJ, 458, 637

Heimdal, H ., Høniger, R ., Jank, J ., & Oberhummer, H ., Gorres, J ., Wiescher, M ., Thielmann, F ., K ., Brown, B . A . 1999, Phys. Rev. C ., 60, 064614

Kajino, T. & Orito, M. 1998, Nucl. Phys. A., 629, 538c

Kajino, T. & Orito, M. 1998, in "Nuclei in the Cosmos V, Proc. 5th International Conference, Volos, Greece, July 6-12, (Editions Frontieres; France), N. P. Rantzos, ed. pp. 17-20.

Kajino, T., Suzuki, T.-K., Kawanomoto, S., & Ando, H. 2000, in The Light Elements and Their Evolution, IAU Symposium Vol 198, L. Da Silva, M. Spite and J. R. de Medeiros, eds. (in press).

Kang, H., & Steigman, G. 1992, Nucl. Phys. B., 372, 494

Kim, J.B., & Lee, H.K. 1995, ApJ, 448, 510

Kim, J.B., Kim J.H., & Lee, H.K. 1998, Phys. Rev. D., 58, 027301

Kinney, W.K. & Riotto, A. 1999, Phys. Rev. Lett., 83, 3366

Ohri, K., Kawasaki, M., & Sato, K. 1997, ApJ, 490, 72

Lange, A. E. et al. 2000, preprint, astro-ph/0005004

Levshakov, S. A., Tytler, D., & Burles, S. 1999, AJ submitted., Los Alamos e-Print Archive., astro-ph/9812114

Lesgourgues, J., Polarski, D. & Starobinsky, A. A. 1999, MNRAS, 308, 281

Lesgourgues, J., Peloso, M. 2000, Phys. Rev., Submitted, astro-ph/0004412

Lesgourgues, J. & Pastor, S. 1999, Phys. Rev. D., 60, 103521

Lineweaver, C. H. & Barbosa, D. 1998, A & A, 319, 799; 1998, ApJ, 496, 624

Lopez, R. E., & Turner, M. S. 1999, Phys. Rev. D., 59, 103502

Lyttleton, R. A., & Bondi, H., 1959, Proc. R. Soc. London. A 252, 313

Mohr, P., Hemdl, H., & Oberhummer, H. 1999 preprint.

Nolett, K. M., & Burles, S. 2000, astro-ph/0001440, submitted to Phys. Rev. D.

Olive, K. A., Schramm, D. N., Thomas, D., & Walker, T. P. 1991, Phys. Lett. B., 265, 239

Olive, K. A. & Steigman, G. 1995, ApJS, 97, 49

Olive, K. A., Steigman, G., & Skillman, E. D. 1997, ApJ, 483, 788

Olive, K. A., Steigman, G., & Walker, T. P. 1999, Phys. Rep. in press.

Orito, M., Kajino, T., & Oberhummer, H. 1998, in "Nuclei in the Cosmos V, Proc. 5th International Conference, Volos, Greece, July 6-12, (Editions Frontieres; France), N. Prantzos, ed. pp. 37-40

Perlmutter, S. et al. 1998a, *Nature*, 391, 51

Perlmutter, S. et al. 1998b, *ApJ*, 517, 565

Piembert, M. & Piembert, A. 2000, in The Light Elements and Their Evolution, IAU Symposium Vol 198, L. D. da Silva, M. Spite and J. R. de Medeiros, eds. (in press).

Primack, J. R., Holtzman, J., Klypin, A., and Caldwell, D. O., 1995, *Phys. Rev. Lett.*, 74, 2160

Riess, A. G. et al. 1998, *AJ*, 116, 1009

Ryan, S. G., Beers, T. C., Olive, K. A., Fields, B. D., & Norris, J. E., 1999, *ApJ*, 530, L57

Scherrer, R. J. 1983 *MNRAS*, 205, 683

Schramm, D. N. & Mathews, G. J. 1995, in Nuclear and Particle Astrophysics in the Next Millennium, ed. E. Kolb, et al. (Singapore: World Scientific), pp. 479-497.

Seljak, U. & Zaldarriaga, M. 1996, *ApJ*, 469, 437

Smith, M. S., Kawano, L. H. & Malaney, R. A., 1993, *ApJS*, 85, 219

Starkman, G. D. 1992, *Phys. Rev. D*, 45, 476

Steigman, G. 2000, astro-ph/0002296

Steigman, G. & Turner, M. S. 1985, *Nucl. Phys. B*, 253, 375

Steigman, G., 1996, *Nucl. Phys. Proc. Suppl.* 48 499.

Terasawa, N., & Sato, K. 1985, *ApJ*, 29, 9

Terasawa, N., & Sato, K. 1988, *Prog. Theor. Phys.*, 80 468

Tytler, D., O'Meara, J. M., Suzuki, N., & Lubin, D. 2000, astro-ph/0001318, to appear in *Physica Scripta*

Wagmans, J., Wagmans, C., Bieber, R., & Geltenbort, P. 1999, astro-ph/9902169

Wagoner, R. V., Fowler, W. A., & Hoyle, F. 1967, *ApJ*, 148, 3

Walker, T. P., Steigman, G., Schramm, D. N., Olive, K. A., & Kang, H. 1991, *ApJ*, 376, 51

White, S. D. M., Navarro, J. F., Evrard, A. E. & Frenk, C. S. 1993, *Nature*, 366, 429.

White, D. A., Fabian, A. C. 1995, *MNRAS*, 273, 72

{ 20 {

Yahil, A., & Beauchet, G. 1976, ApJ, 206, 26

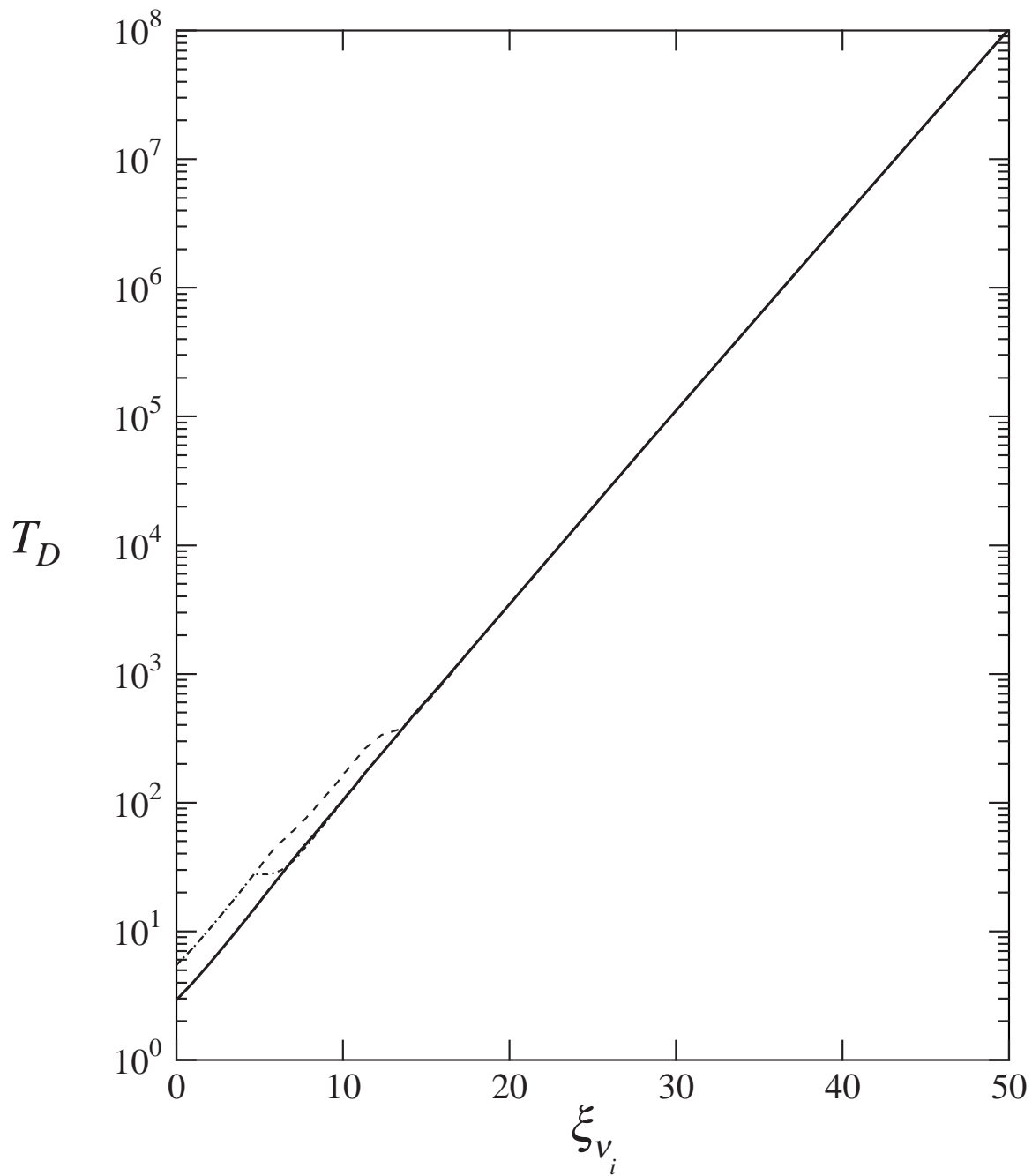


Fig. 1. Decoupling temperature T_D (in MeV) for: e^- (solid line); ν_e (dot-dashed line); and ν_i (dashed line) as a function of degeneracy parameter ξ_{ν_i} .

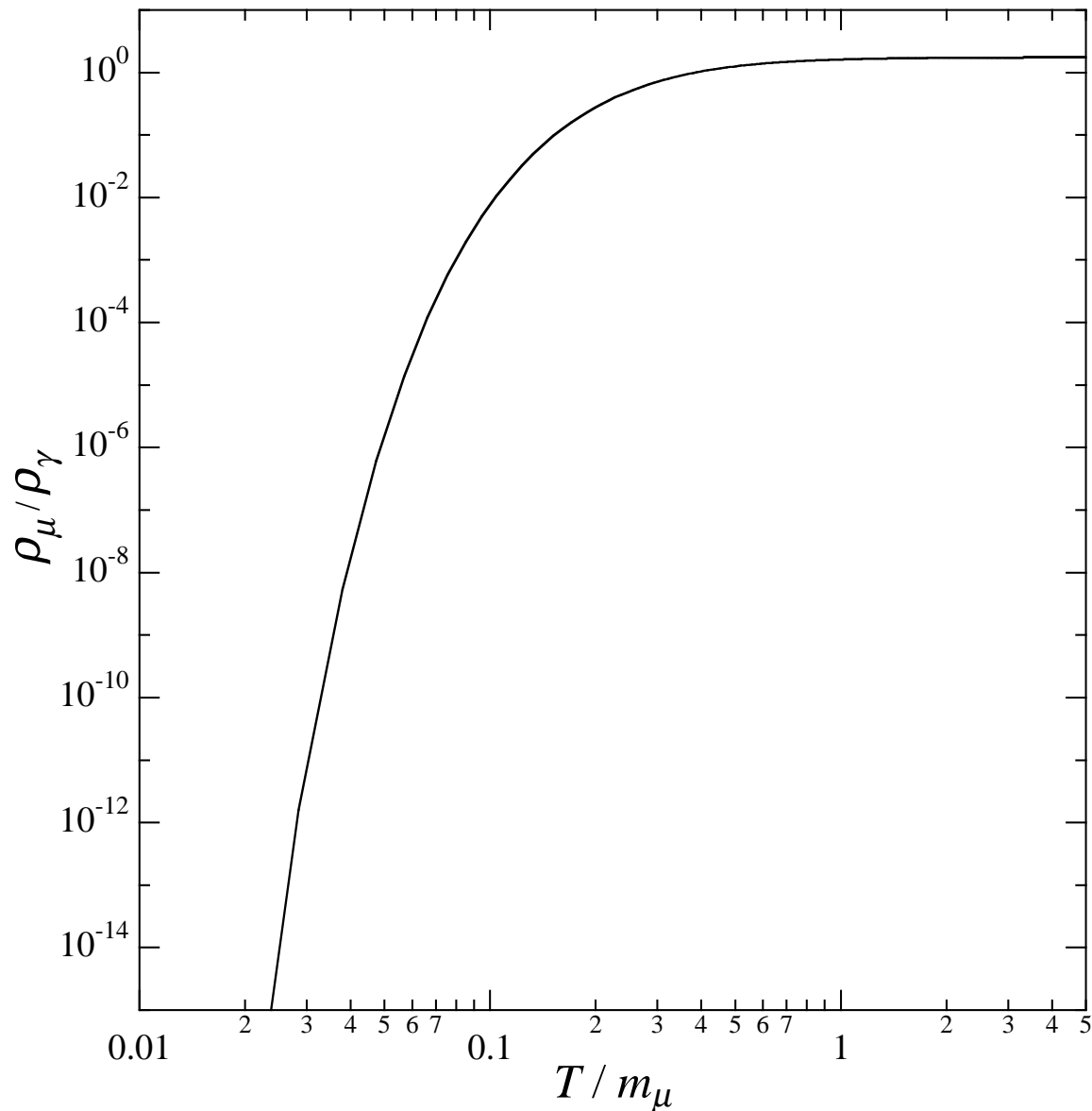


Fig. 2.1 Ratio of the energy density of muons (or any massive particle) to photons as a function of the ratio of temperature to rest mass. This shows that even at a temperature of only 20% of the rest mass, a significant fraction (10%) of the energy density still resides in particle/antiparticle pairs.

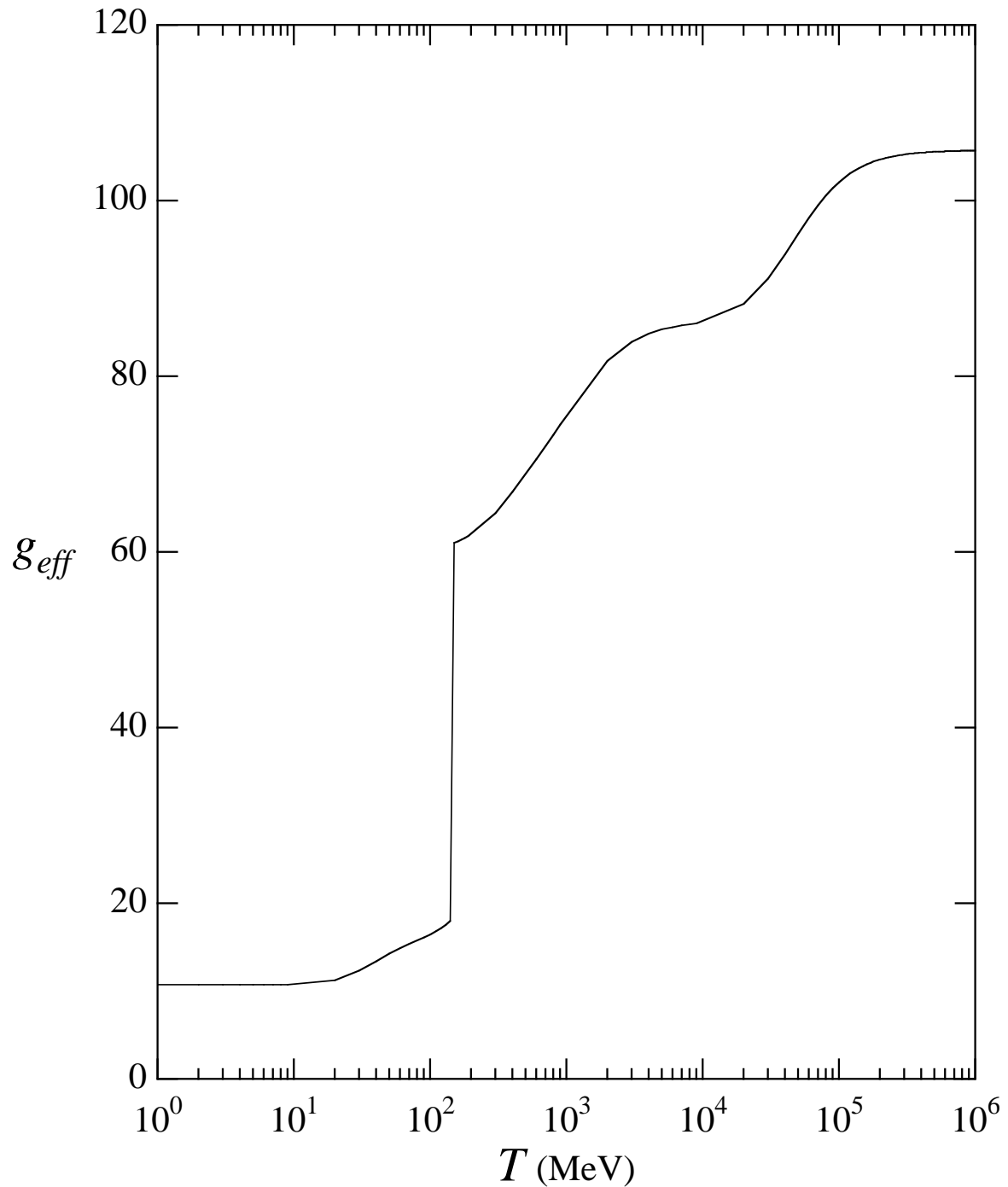


Fig. 3. Effective degrees of freedom g_{eff} as a function of temperature. The discontinuity at $T = 150$ MeV is due to the QCD phase transition.

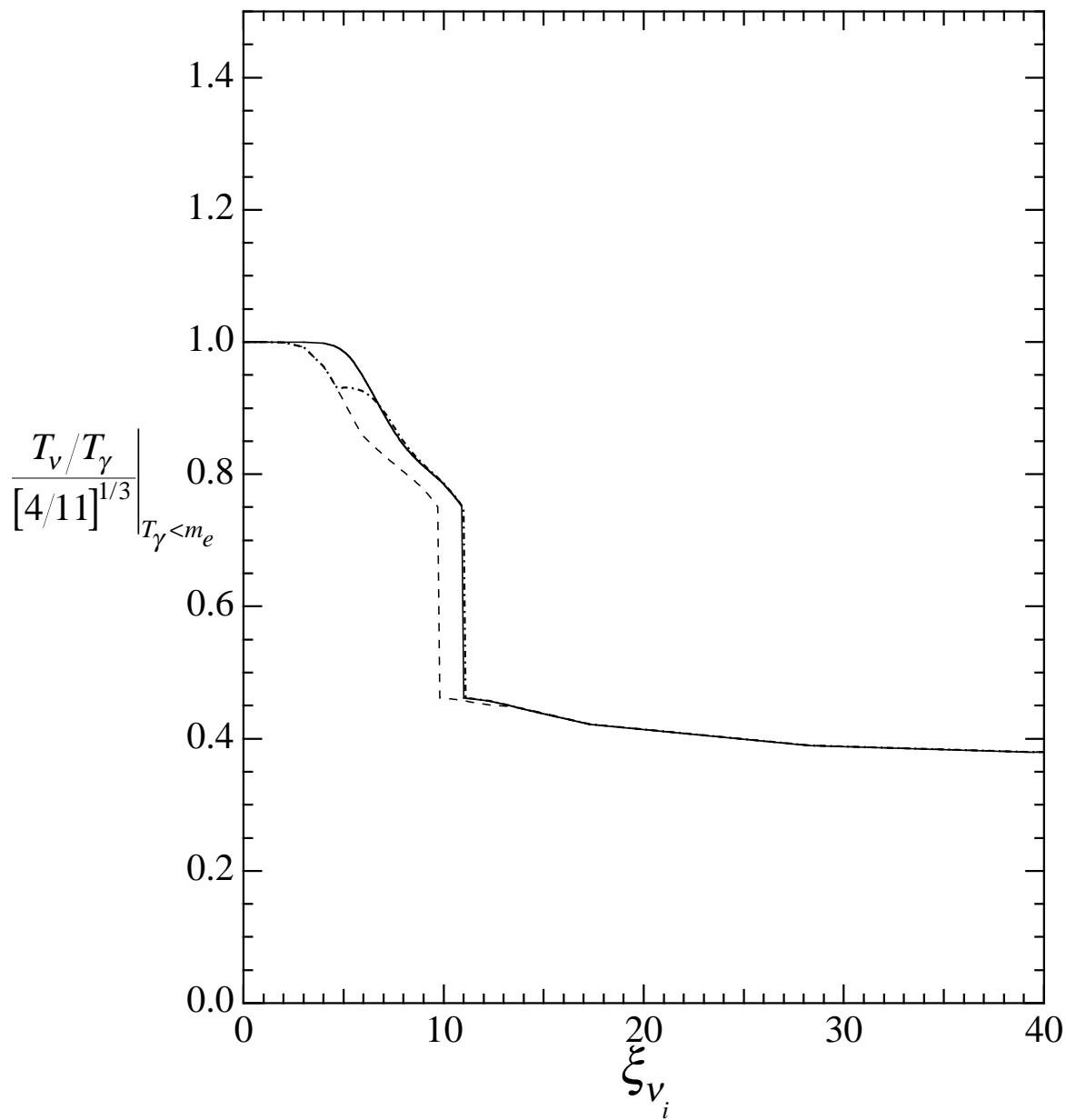


Fig. 4. | Ratio of relic neutrino temperature to photon temperature as a function of degeneracy parameter for each neutrino species; ν_e (solid line), ν_μ (dot-dashed line), ν_τ (dashed line).

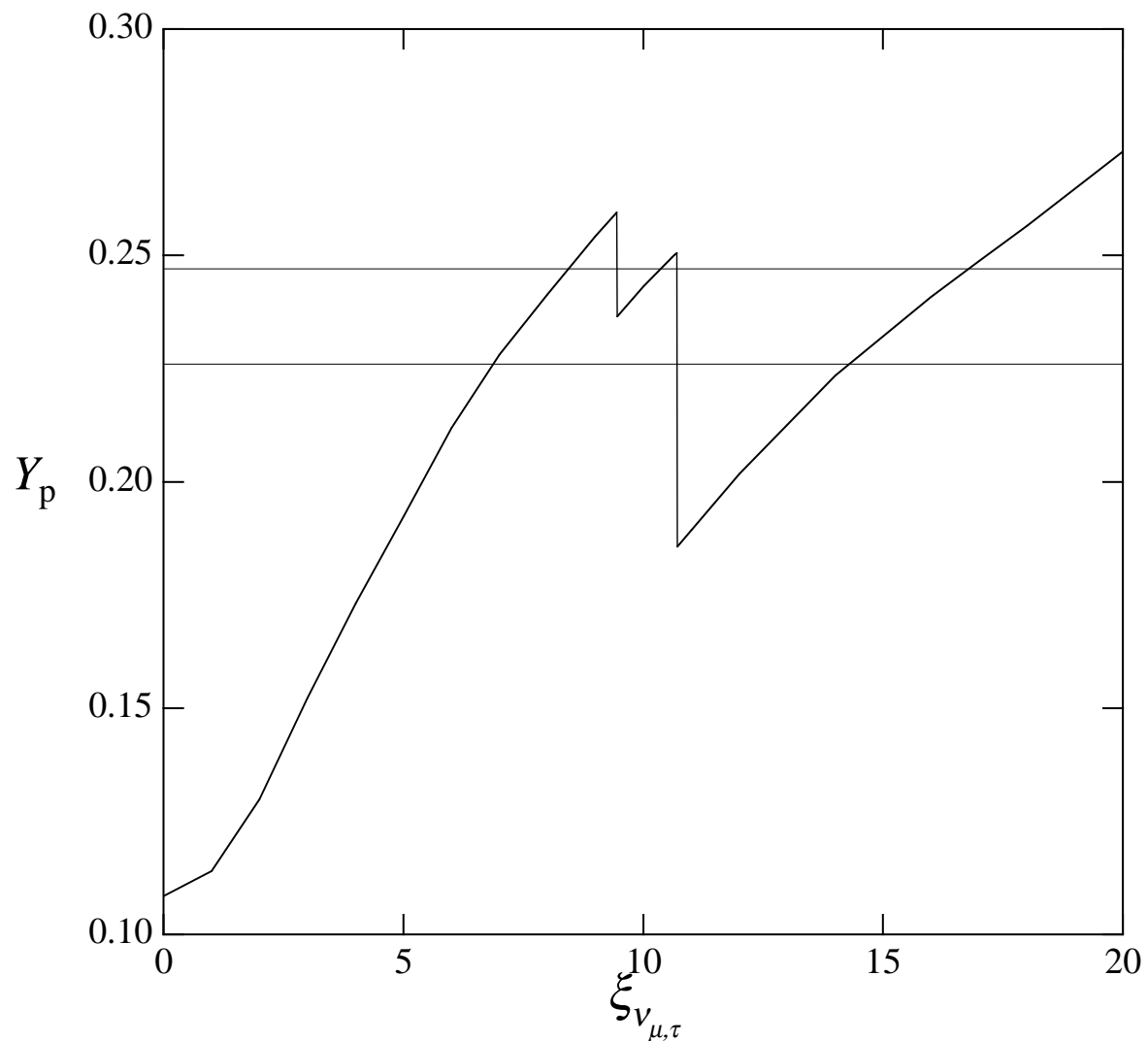


Fig. 5. Helium mass fraction Y_p as a function of degeneracy parameter $\xi_{\nu_{\mu,\tau}}$, for $bh_{50}^2 = 0.3$ and $\epsilon = 0.8$. Horizontal lines show the adopted observational constraints.

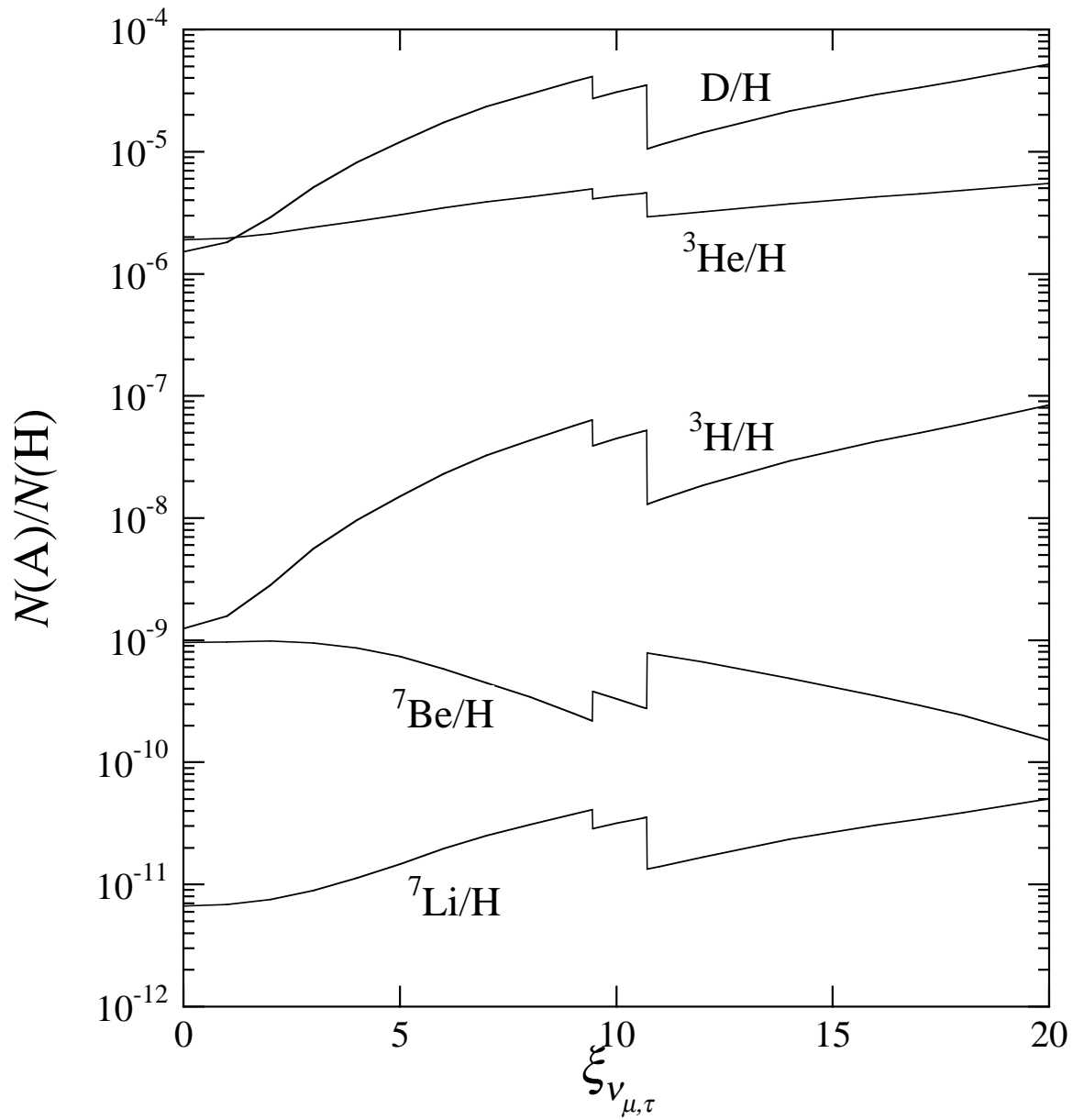


Fig. 6. The predicted abundances of the light elements as a function of the neutrino degeneracy, for $bh_{50}^2 = 0.3$ and $\epsilon = 0.8$.

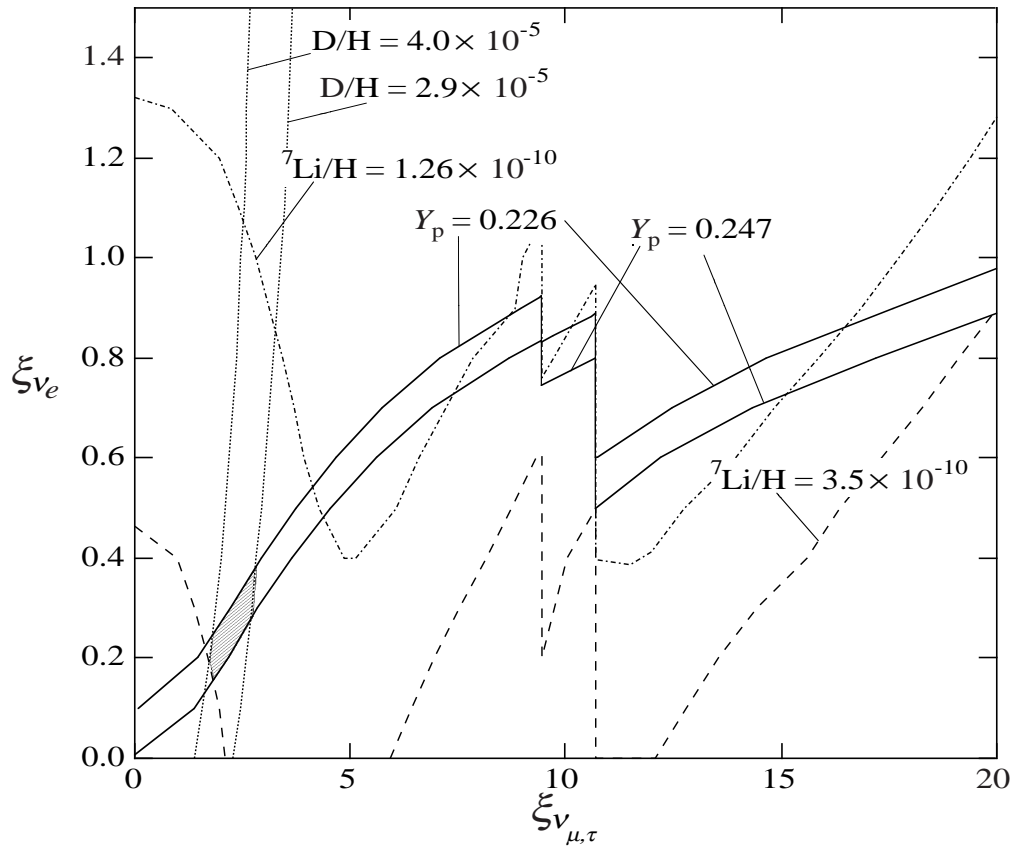


Fig. 7(a).| Contours of allowed values in the ξ_{ν_e} , $\xi_{\nu_{\mu,\tau}}$ plane for $\text{b}h_{50}^2 = 0.1$, based upon the various light-element abundance constraints as indicated. The hatched region depicts the allowed parameters consistent with all light element constraints for this value of $\text{b}h_{50}^2$.

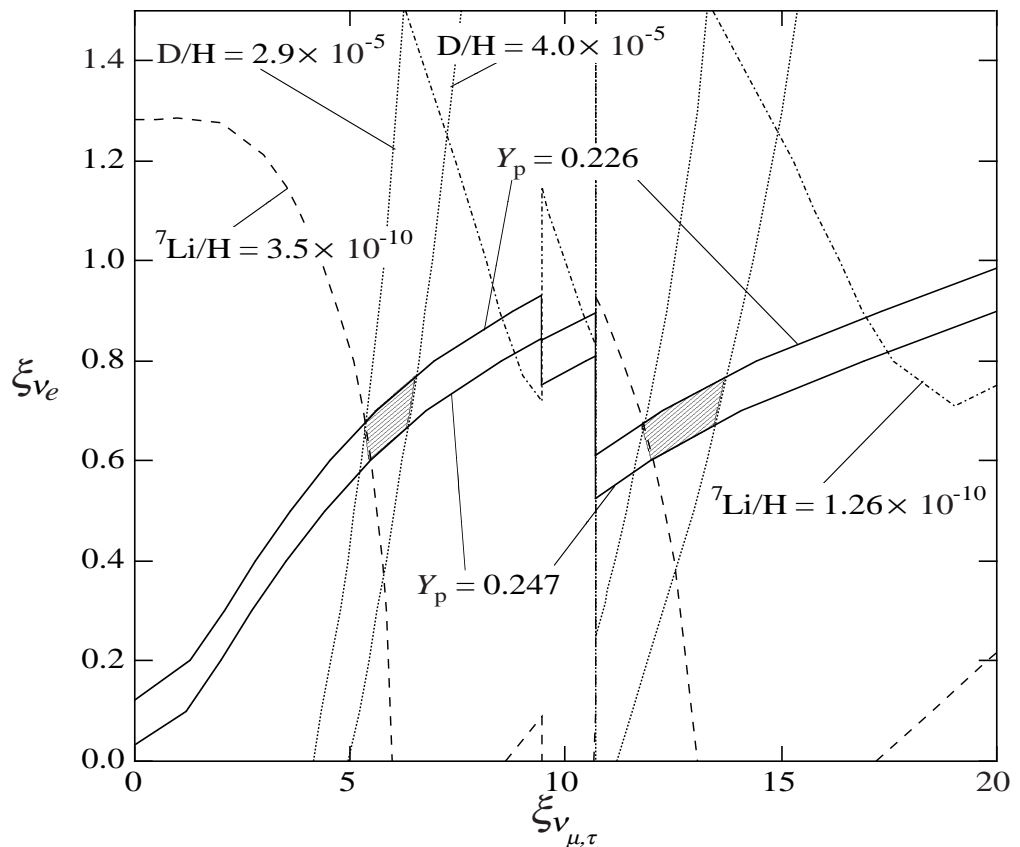


Fig. 7(b).| Same as Fig. 7a, but for $b h_{50}^2 = 0.2$.

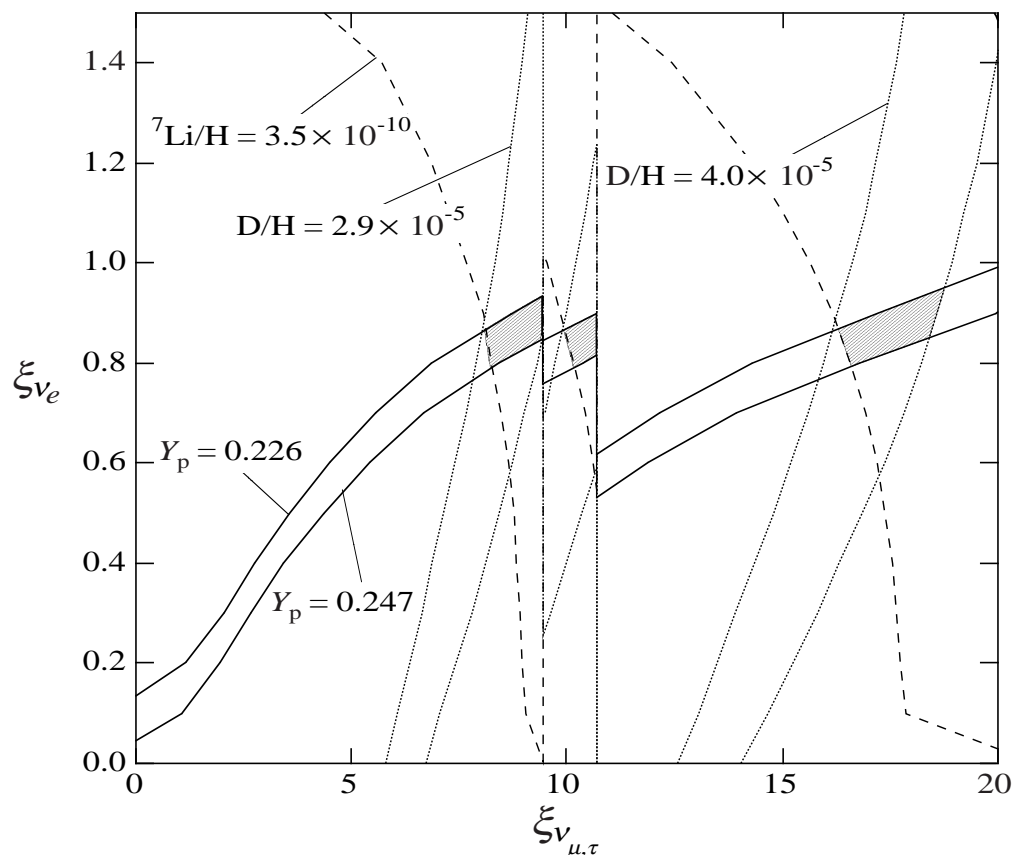


Fig. 7 (c).| Same as Fig 7a, but for ${}_{\text{b}}\text{h}_{50}^2 = 0.3$.

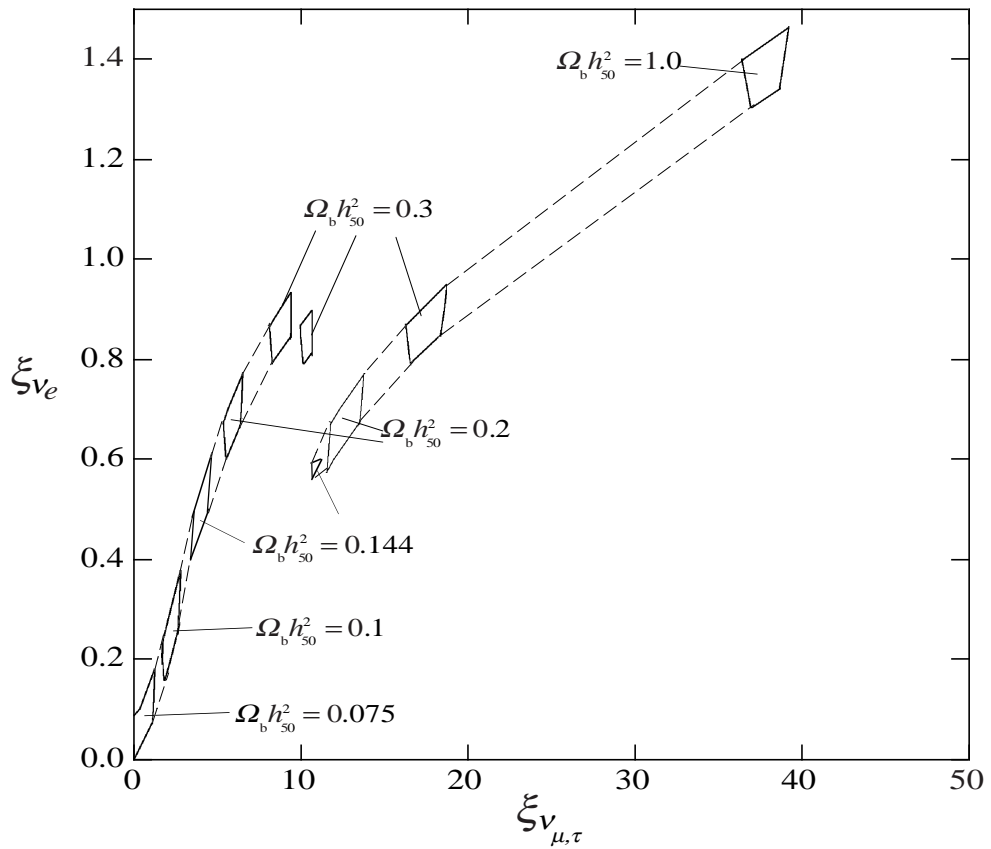


Fig. 8. | Allowed values of ξ_{ν_e} and $\xi_{\nu_{\mu,\tau}}$, for which the constraints from light element abundances are satisfied for values of $\Omega_b h_{50}^2 = 0.075, 0.1, 0.144, 0.2$, and 0.3 as indicated. For large values of $\Omega_b h_{50}^2 > 0.3$ the only allowed regions are for the large values $\xi_{\nu_{\mu,\tau}} > 20$.

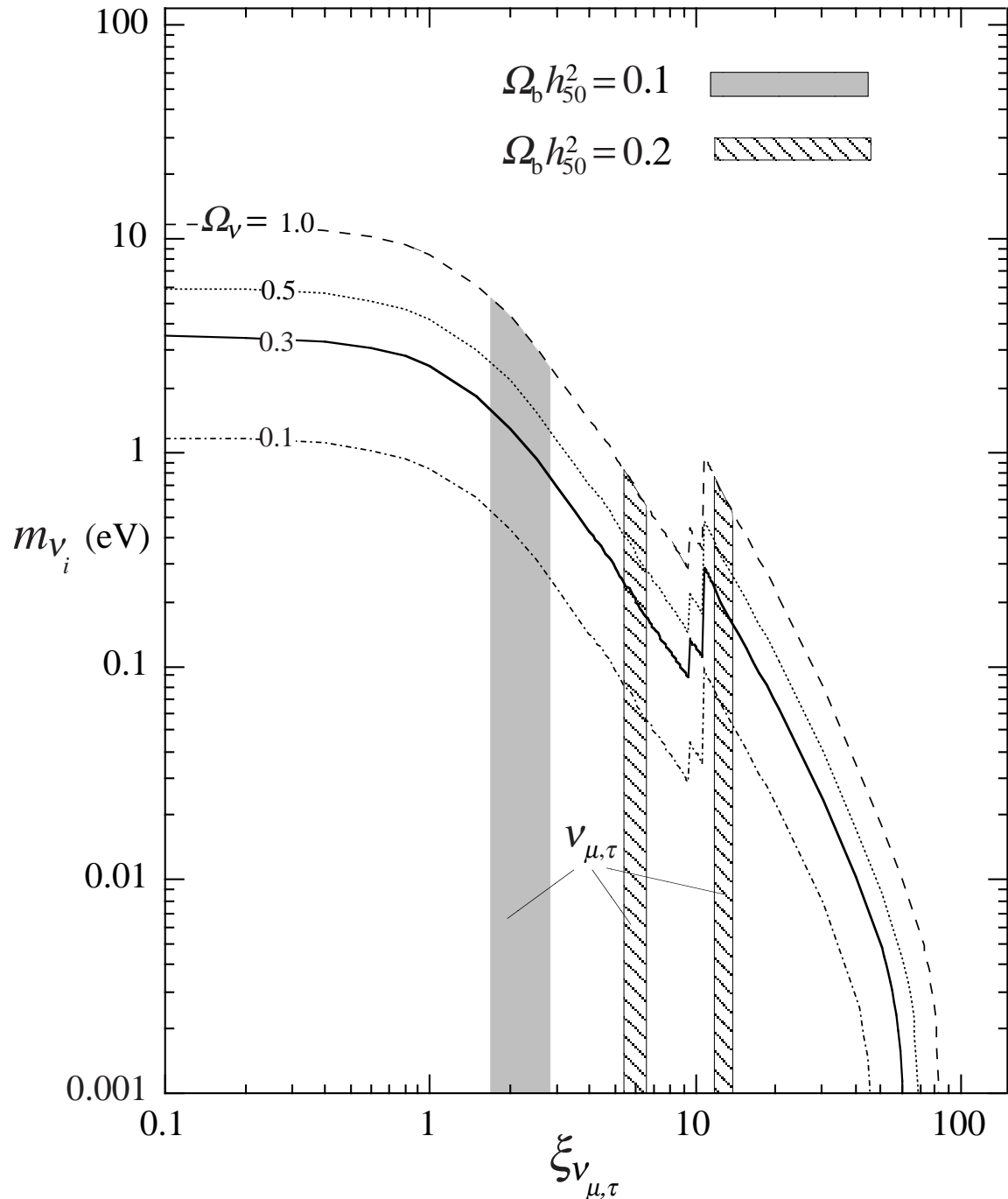


Fig. 9. | Contours of equal present energy density of massive degenerate neutrinos as a function of the degeneracy $\xi_{\nu_{\mu,\tau}}$ and neutrino mass m_{ν_i} for $\Omega_\nu = 0.1, 0.3, 0.5$, and 1.0 as indicated. Each curve corresponds to different value of Ω_ν as indicated. Shaded regions depict the allowed range of degeneracy for the two indicated values of $\Omega_b h_{50}^2 = 0.1$, and 0.2 as shown in Fig. 8.

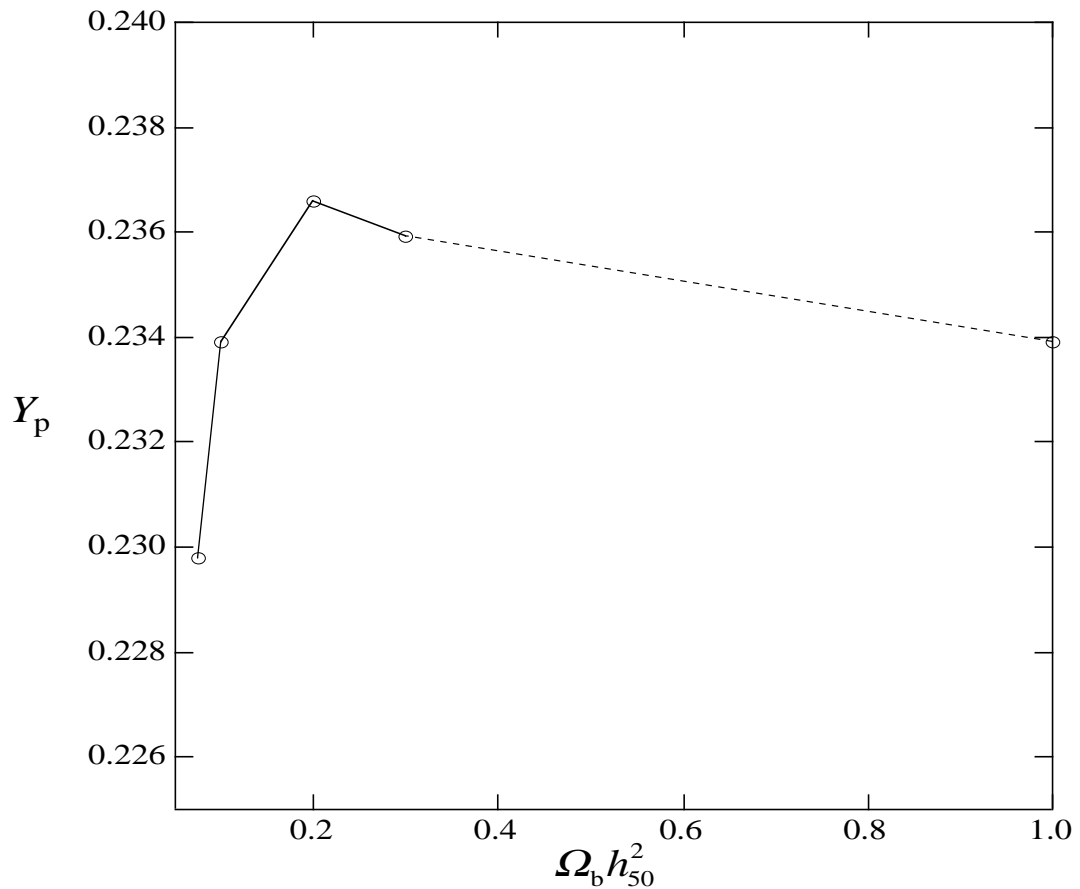


Fig. 10. The predicted Helium abundance for allowed neutrino-degenerate models as a function of $\Omega_b h_{50}^2$. The values of Ω_b and h_{50} were taken from the central value in the allowed region determined by $\Omega_b h_{50}^2$ in Fig. 8.

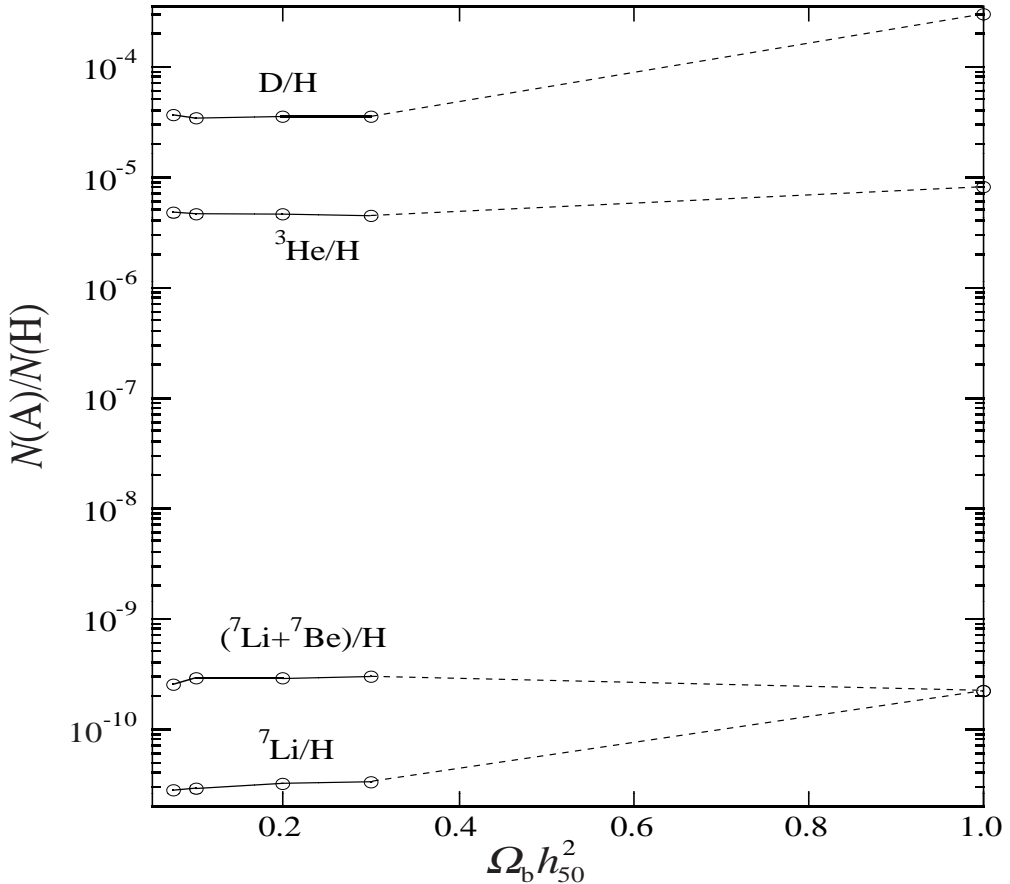


Fig. 11. The predicted D/H , $^3\text{He}/\text{H}$, and total $\text{A} = 7$ and ^7Li abundances for allowed neutrino-degenerate models as a function of $\Omega_b h_{50}^2$. The values of Ω_b and h_{50} were taken from the central value in the allowed region determined by $\Omega_b h_{50}^2$ in Fig. 8.

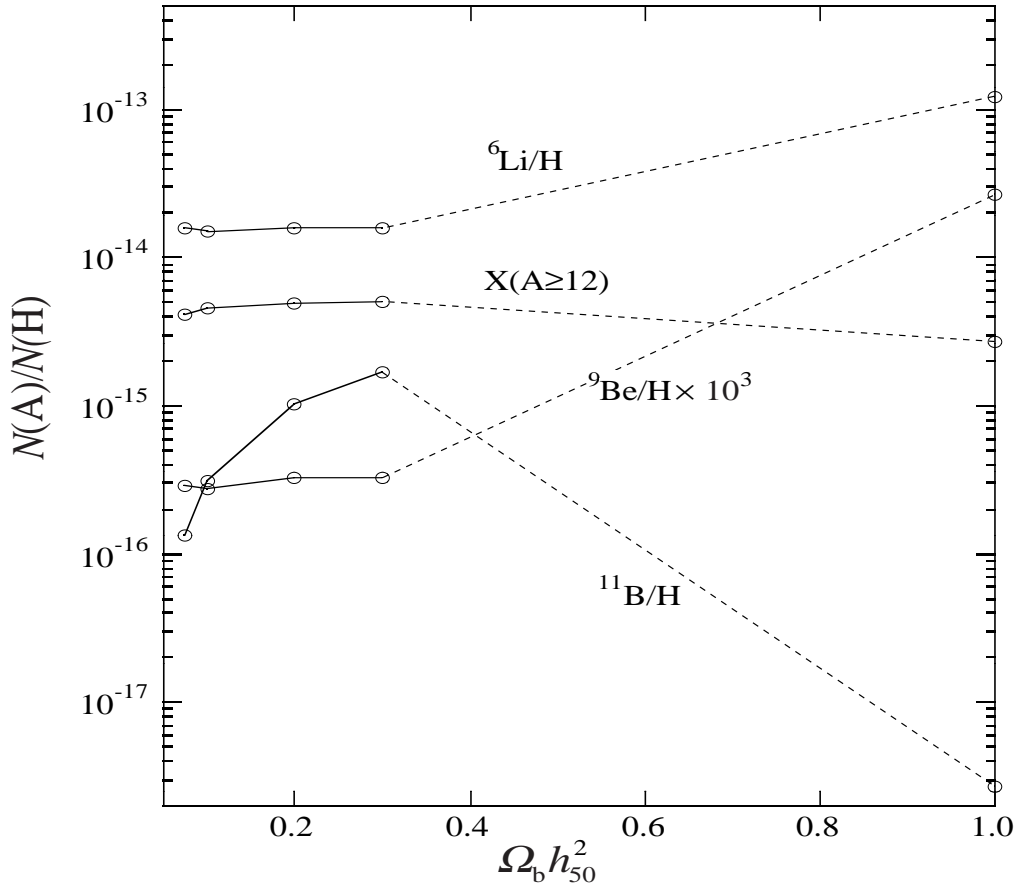


Fig. 12. The predicted ${}^6\text{Li}$, ${}^9\text{Be}$, ${}^{11}\text{B}$ and $X(A \geq 12)$ abundances as a function of $\Omega_b h_{50}^2$. The values of Ω_b and h_{50} were taken from the central value in the allowed region determined by $\Omega_b h_{50}^2$ in Fig. 8.

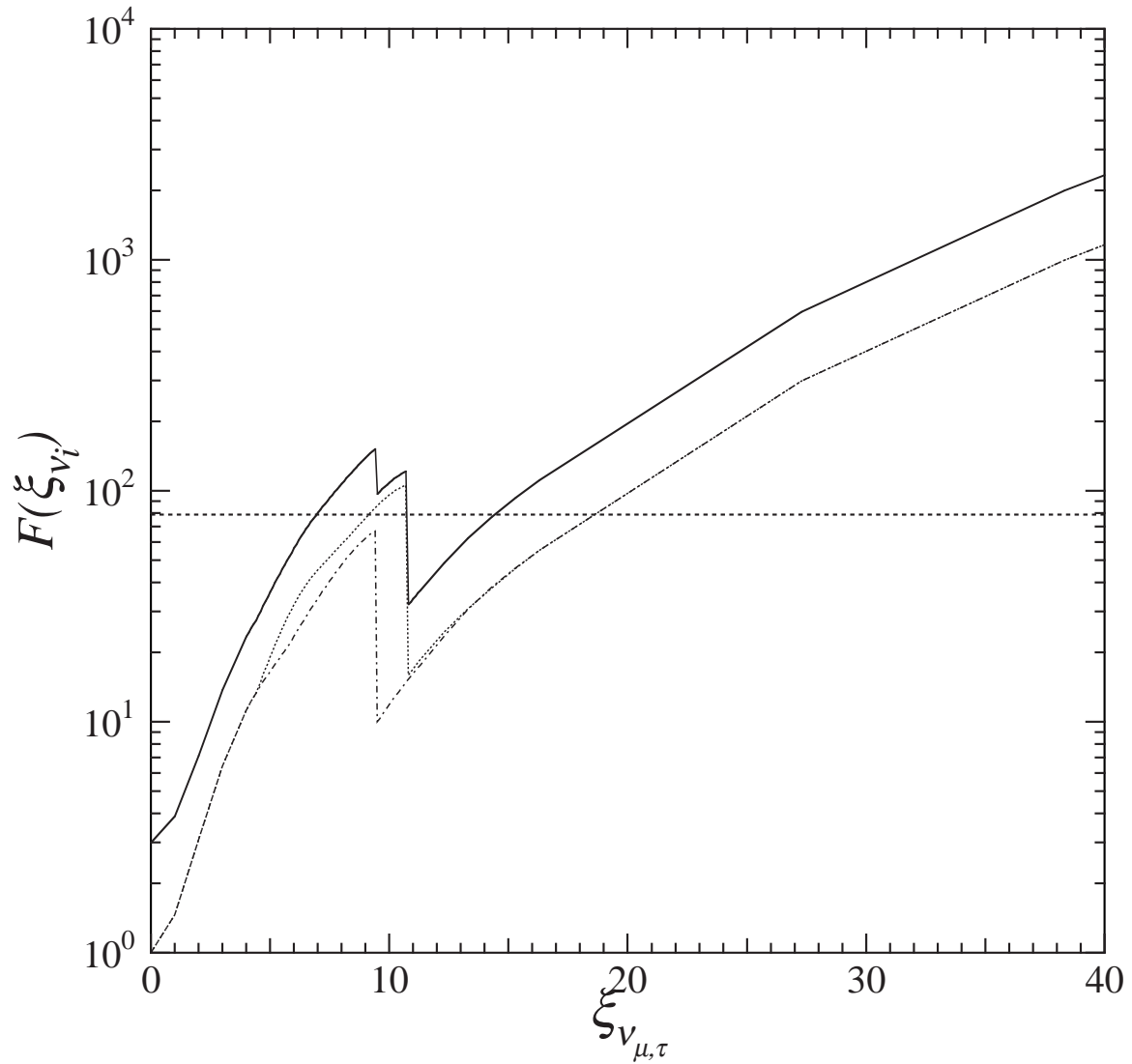


Fig. 13. | Calculated neutrino energy density factors $F(\xi_i)$ as a function of degeneracy parameter for the three neutrino species. The dotted and dot-dashed curves display respectively $F(\xi)$ and $F(\xi)$ for the cases in which only one neutrino species is degenerate. Since our interesting parameter regions in Figure 8 satisfy $\xi_e \gg \xi_\mu, \xi_\tau$, only ξ_μ, ξ_τ contribute significantly to the total $F(\xi)$ (solid curve). The dashed horizontal line indicates the constraint on neutrino degeneracy from the requirement that sufficient structure develops by the present time.

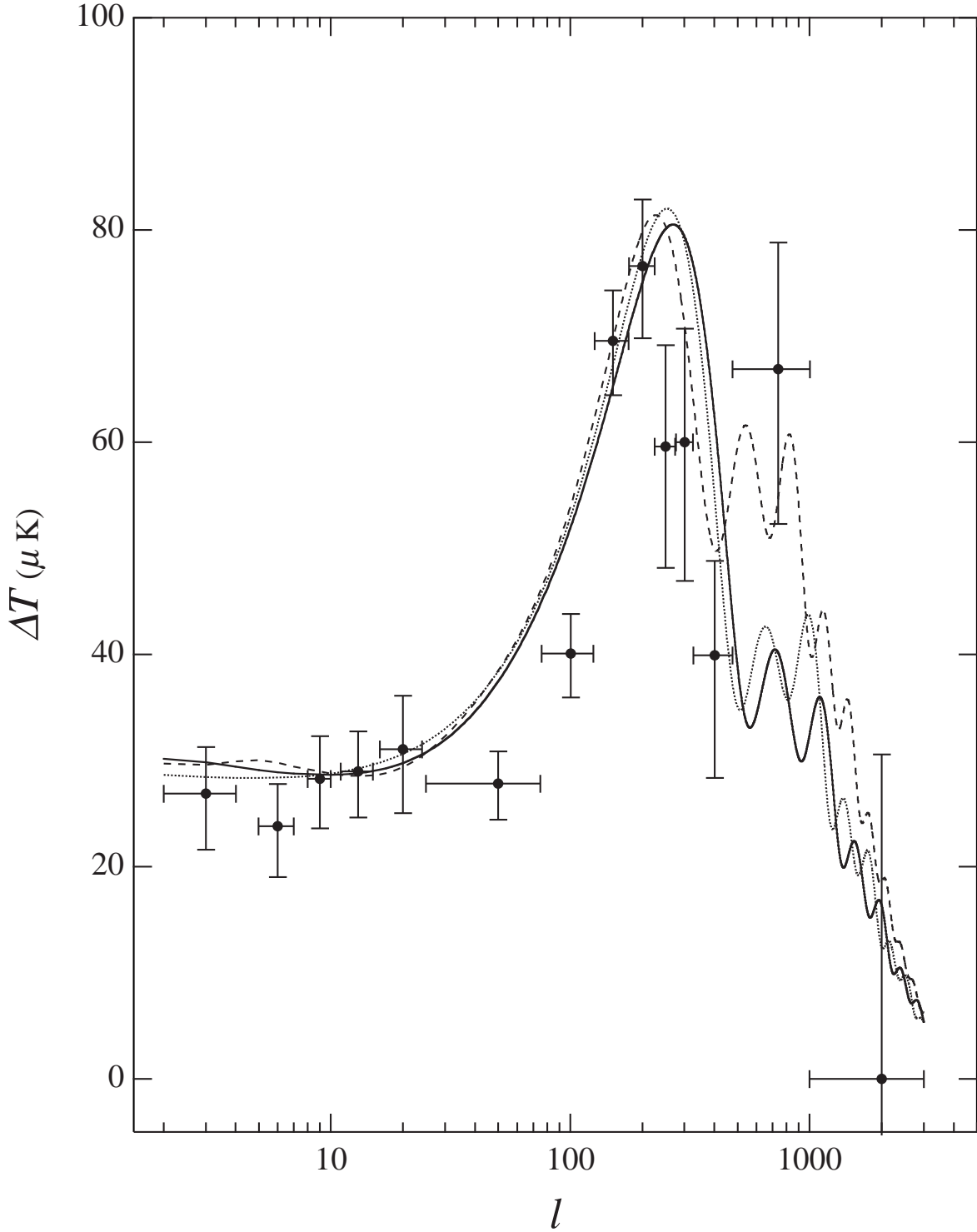


Fig. 14.1 CMB power spectrum compared with calculated $\Omega = 1$ models. The points show the binning of 69 experimental measurements based upon the radical compression method of Bond et al. (2000). The dashed line shows the optimum model of Dodelson & Knox (2000). The solid line shows an $\Omega = 0.4$ model with three degenerate neutrinos, $\Omega_b = 10:7$, $\Omega_c = 0.58$ as described in the text. The dotted line is for an $\Omega = 0$ model with the same degeneracy parameters.

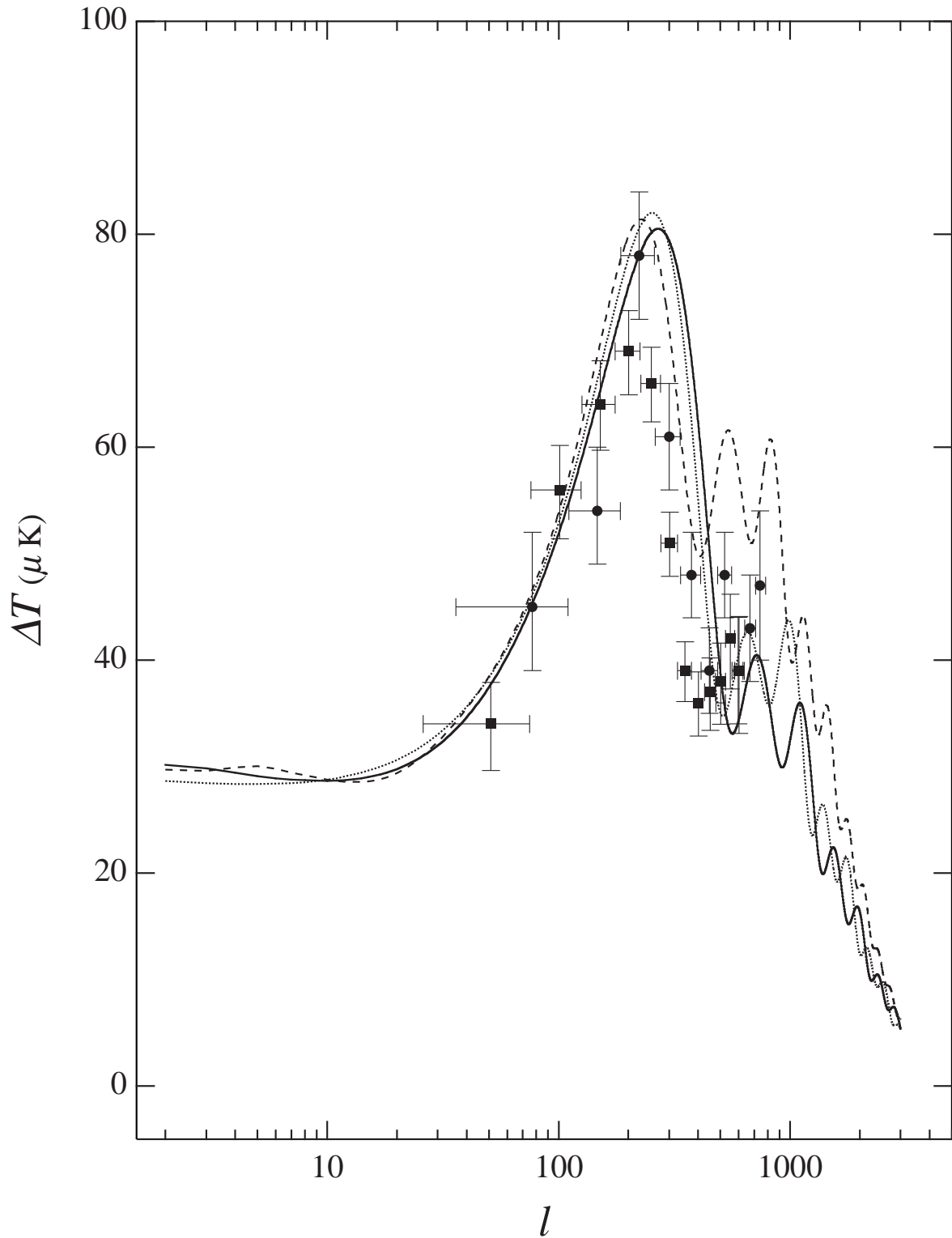


Fig. 15.1 CMB power spectrum from the recent MAXIMA-1 (circles) and BOOMERANG (squares) MAXIMA-1 (circles) binned data compared with calculated $\Lambda = 1$ models of Figure 14. Note that the suppression of the second acoustic peak in the data is consistent with that predicted by the neutrino-degenerate models.